AERO-ACOUSTIC EXPERIMENTAL VERIFICATION OF OPTIMUM CONFIGURATION OF VARIABLE-PITCH FANS FOR 40 x 80 FOOT SUBSONIC WIND TUNNEL

FINAL REPORT

(NASA-CR-152040) AERO-ACOUSTIC EXPERIMENTAL VERIFICATION OF OPTIMUM CONFIGURATION OF VARIABLE-PITCH FANS FOR 40 X 80 FOOT SUBSONIC WIND TUNNEL Final Report (General Electric Co.) 65 p HC A04/MF A01 CSCL 14B G3/09

N78-10115

Unclas

52030

Prepared for

NASA-AMES RESEARCH CENTER
MOFFETT FIELD, CALIFORNIA

Contract No. NAS2-8364
CR-152,040

Prepared by

Harold Lown
Applied Mechanics Branch
Power Generation and Propulsion Laboratory
Corporate Research and Development
General Electric Company
Schenectady, New York 12301

August 1977

SRD-77-133

AERO-ACOUSTIC EXPERIMENTAL VERIFICATION OF OPTIMUM CONFIGURATION OF VARIABLE-PITCH FANS FOR 40 x 80 FOOT SUBSONIC WIND TUNNEL

FINAL REPORT

Prepared for

NASA-AMES RESEARCH CENTER
MOFFETT FIELD, CALIFORNIA

Contract No. NAS2-8364
CR-152,040

Prepared by

Harold Lown.
Applied Mechanics Branch
Power Generation and Propulsion Laboratory
Corporate Research and Development
General Electric Company
Schenectady, New York 12301

August 1977

FOREWORD

This final report, "Aero-Acoustic Experimental Verification on Optimum Configuration of Variable Pitch Fans for 40 x 80 Foot Subsonic Wind Tunnel," covers the work completed under NASA Contract NAS2-8364 for NASA-Ames Research Center, Moffett Field, California. The work was performed by both the Applied Mechanics Branch in the Power Generation and Propulsion Laboratory of Corporate Research and Development (CRD) and the Compressor Aerodynamic Section of the Aircraft Engine Business Group (AEBG) of the General Electric Company. The principal contributors to the program were:

H. Lown, CRD

M.R. Simonson, AEBG

Dr. L.H. Smith, Jr., AEBG

R.J. Wells, CRD

TABLE OF CONTENTS

PRECEDING PAGE BLANK NOT FILMED

TABLE OF CONTENTS (Cont'd)

LIST OF ILLUSTRATIONS

LIST OF TABLES

Section 1

INTRODUCTION

Corporate Research and Development (CRD) of the General Electric Company has since 1970 been involved in a series of fan design studies and a model fan test verification program in aiding the National Aeronautics and Space Administration to achieve optimum aero-acoustic performance on new variable pitch fans to be incorporated into the repowered drive section of the 40 x 80 foot wind tunnel at Moffett Field, California. The previous design studies (Refs. 1-5) established the basis for design, construction, and test program for the 1/7-scale model fan conducted by NASA-Ames to verify the 40 foot full-scale fans to be incorporated in the repowered section of the 40 x 80 foot wind tunnel.

This report describes the results of the several phases involved in the "40 x 80 Foot Subsonic Wind Tunnel Fan Section Verification Program" employing 1/7-scale model fans, conducted by General Electric under Contract NAS2-8364. The objective and scope of this contract were to monitor the aerodynamic and acoustic performance of the two fan configurations under investigation (low-speed and high-speed variable pitch fan design), supply the necessary aero-acoustic data-reduction computer program logic, evaluate the results of the tests, and recommend the optimum configuration to be employed in the final 40 foot full-scale fan.

The original design of the low-speed and high-speed fans and the test vehicle for the 1/7-scale model fan were previously reported on in Reference 5. The test program was therefore a continuation of that program, designed to verify how well the fans met the design objectives and also the ability of the fans to operate with large inlet boundary layer growth, such as is present in the wind tunnel power section of the full-scale fans.

The initial 1/7-scale model fan test results showed that the noise generated by the low-speed model fan configuration when scaled to its full-scale configuration would be 5 dBA quieter than the high-speed fan configuration. The aerodynamic test program became focused then on the low-speed fan model. As the low-speed model fan tests progressed, however, it became apparent that the low-speed fan design would have serious problems in meeting the wind tunnel airflow objectives, especially if a lower hub/tip ratio fan design were incorporated in the full-scale fans.

The original contract was therefore expanded in scope to include a restudy effort on the low-speed fan model. General Electric's Aircraft Engine Business Group (AEBG) Compressor Aerodynamic Section was involved in this phase of the contract, evaluating the fan operating characteristics with a lower hub/tip ratio and more severe inlet boundary layer condition. The results of the new fan study and recommendations leading to improved low-speed fan performance have also been incorporated in this report.

WIND TUNNEL FAN OPERATING REQUIREMENTS

In structuring the model fan test program, careful consideration had to be given to all the operating requirements imposed on the variable-pitch fans of the repowered wind tunnel. The new power section described schematically in Figure 1 is designed to operate with both a closed and an open wind tunnel configuration. The previous GE study (Ref. 4) evolved the fan design operating requirements for these two tunnel configurations which are shown in Table 1.

Table 1

FULL-SCALE FAN AERODYNAMIC DESIGN CONDITIONS

Parameter	Closed Tunnel Configuration	Open Tunnel Configuration
Inlet Total Pressure (psia)	14.54	14.55
Inlet Total Temp. (^{o}R)	530	530
Fan Weight Flow (lb/sec)	16333	20251
Fan Head Rise (ft)	680	525
Fan Stage Efficiency (%)	90	86
Fan Head Input (ft)	756	610
Fan Tip Diameter (ft)	40	40
Hub/Tip Ratio	0.5	0.5
Fan Rpm	180	180

These design conditions, derived from the motor drive power output limitation of 135,000 hp for the existing power section of the 40 x 80 foot wind tunnel, resulted in attaining tunnel test section speeds of 300 knots and 102 knots, respectively, for the closed and open tunnel configurations.

The variable-pitch fan capability was in turn designed to permit attaining various closed tunnel speeds ranging in value from 58 to 100 percent of design, while maintaining the synchronous fixed speed of the motors.

The fan arrangement in the power section shown in Figure 1 results in large boundary-layer generation at the inlet to the corner fans, where the two wall boundary layers merge. This produces sizable inlet velocity profile distortions that can result in fan stall. In order to assess the effect of large in-flow distortions, the fan model experimental program was designed to include investigation of fan performance with different degrees of distorted inlet profiles, artificially generated.

Another important consideration in the fan model experimental program was the evaluation of the likelihood of fan stall and performance deterioration if a lower hub/tip ratio of 0.4375 were employed in the final full-scale fan design. On the basis of NASA-Ames studies a gain of approximately 6 percent in tunnel speed could be affected by going from a fan hub/tip ratio of 0.5 to 0.4375. This improvement in tunnel performance results from the reduced diffuser losses downstream of the fan, affected by a smaller fan center body.

FAN ACOUSTIC PROGRAM

The basic objective of the fan acoustic program was to verify the theoretically calculated acoustic advantage of utilizing a low-speed fan over that of a high-speed fan in the power section of the 40 x 80 foot wind tunnel. This theoretical advantage was estimated to be in the order of 13.2 dBA in lower noise for the six prototype low-speed fans versus the six prototype high-speed fans, or a total sound power level of 139 dBA versus 152.6 dBA. The actual fan noise was in turn to be established experimentally by obtaining the third-octave band noise frequency spectrum with an array of microphone settings covering the inlet and discharge duct cross-sectional areas.

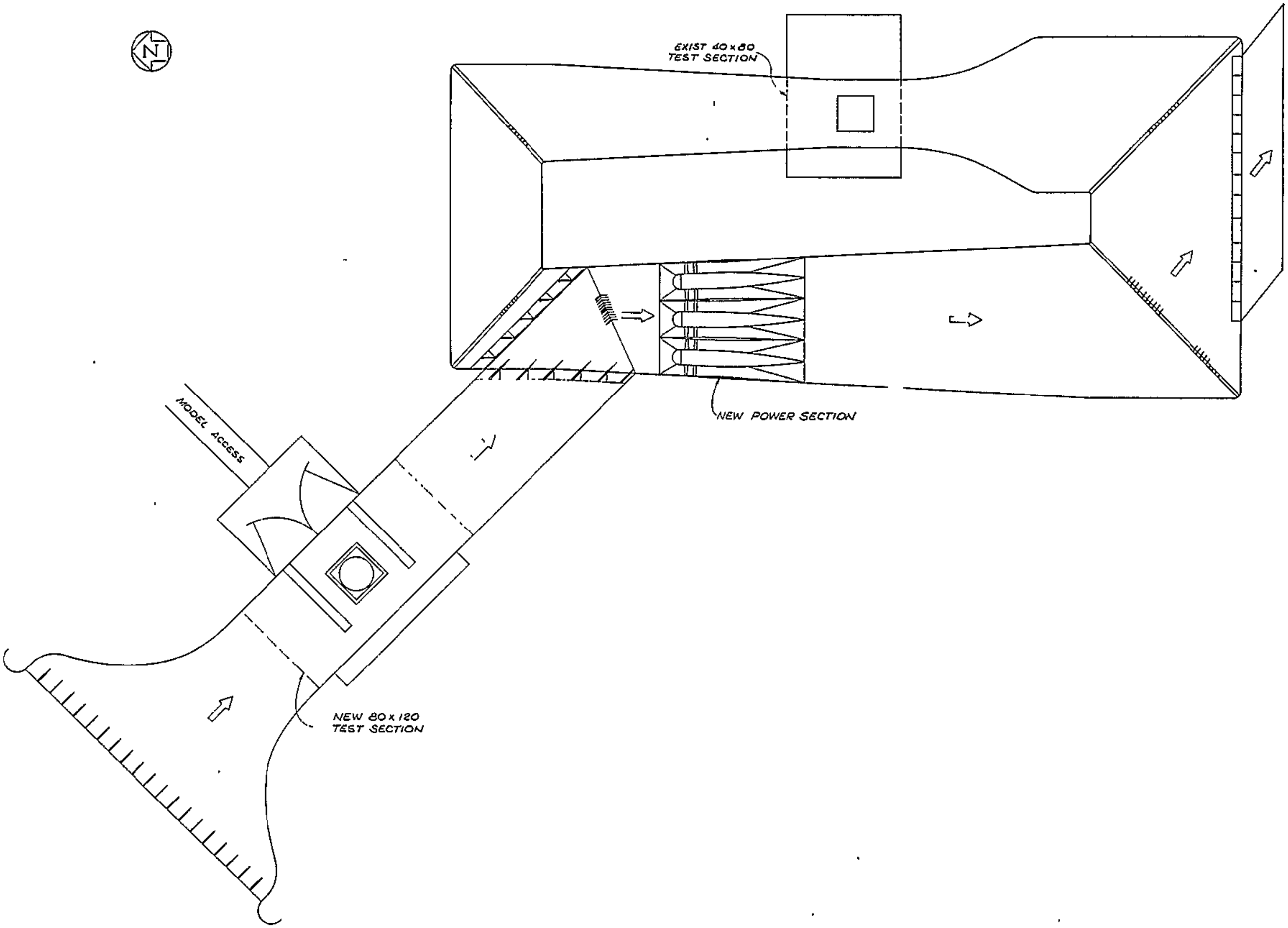

Figure 1. New 40 x 80 Foot Wind Tunnel Power Section

PRECEDING PAGE BLANK NOT FILMED

Section 2

1/7-SCALE MODEL FAN EXPERIMENTAL PROGRAM PRETEST PHASE

The 40 x 80 foot aero-acoustic verification program was to be carried out at NASA-Ames with the 1/7-scale test model shown in Figure 2. The pretest phase of this program included designation of the aero-acoustic instrumentation and development of the aero-acoustic data-reduction computer programs to be employed during the tests.

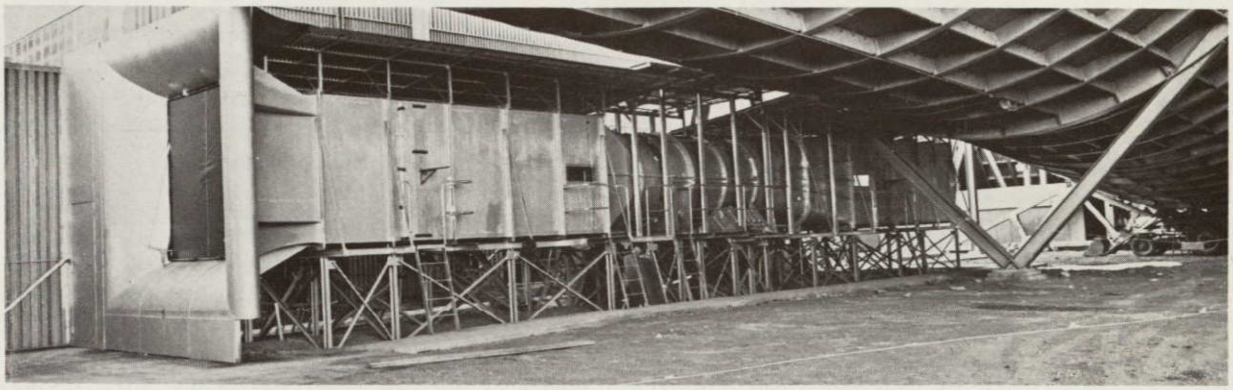

Figure 2. 1/7-Scale Model Fan Test Vehicle

INSTRUMENTATION

The instrumentation designed to obtain the model fan aero-acoustic performance consisted of static pressure instrumentation, total pressure rakes, a combined total pressure/static pressure/directional survey probe, and a four-microphone traversing rod as well as temperature, speed, and torque measuring instrumentation. The inlet bellmouth section of the test vehicle was employed as the weight flow metering device. The complete arrangement of the test vehicle instrumentation, the designated measuring stations, and their exact axial location are presented in the instrumentation schematic of Figure 3.

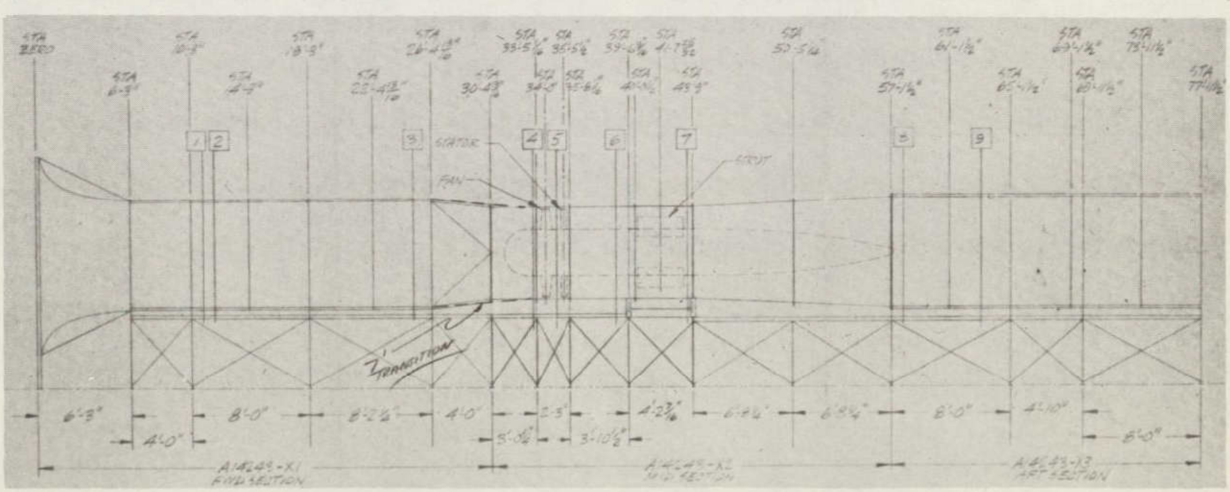

Figure 3. Instrumentation Schematic

Aerodynamic Instrumentation

The aerodynamic instrumentation required to obtain either fan overall aerodynamic performance, detailed rotor performance, or diffuser performance is presented in Appendix A of this report. While the instrumentation section dealing with fan overall performance (Section A of Appendix A) shows four circumferential positions at Station 6 for obtaining the radial distribution in fan performance, only one traversing probe was available for the tests. This required physically moving the probe to each of the four azimuth positions; therefore each position of the traversing probe represented a different test even though the flow and speed settings were the same.

Inlet Bellmouth Weight Flow Calibration Tests

To employ the bellmouth section of the fan test vehicle as a weight flow measuring nozzle, its flow coefficient had to be established. The high Reynolds number of the bellmouth throat section of 4×10^6 readily lent itself to obtaining its flow coefficient with a scaled model, since the lower Reynolds number of the scaled model would still be sufficiently high not to affect the flow coefficient accuracy.

A bellmouth model having a 1 ft^2 throat section was manufactured, and weight flow calibration tests were conducted at CRD. The metering flow nozzles employed in obtaining the bellmouth flow coefficient had a high degree of accuracy, approaching a flow coefficient of 0.998.

The results of the bellmouth section calibration tests showed that for throat Reynolds numbers of 10^6 or greater, the test vehicle bellmouth section would have a flow coefficient CN of 0.989.

Acoustic Instrumentation

The acoustic instrumentation was designed to obtain the inlet and discharge fan noise spectra at stations 2 and 9 (Figure 3) respectively. A continuous microphone traversing system of employing two probe-mounted microphones 45° apart was initially recommended. Because of mechanical complexity, however, a traversing discreet-position microphone system consisting of four microphones on a movable strut was used. The sound power was obtained by subdividing the inlet and discharge ducts into 36 equally spaced cells and measuring the noise spectra in each of these cells with the four-microphone-array measuring probe. The microphone probe is shown in Figure 4, the nine locations of the microphones necessary to obtain either fan intake or exhaust noise for each test point are shown in Figure 5.

AERODYNAMIC AND ACOUSTIC PERFORMANCE DATA REDUCTION

The fan aerodynamic and acoustic test data reduction was a joint effort carried out by CRD and NASA-Ames. In the case of fan aerodynamic data reduction CRD provided the computational logic required to structure a computer program that would develop the detailed fan performance. The actual data reduction was conducted by NASA-Ames. In the case of fan noise reduction, the noise measurements were recorded on tape by NASA-Ames and transmitted to CRD for final reduction on the General Radio real-time analyzer, and the associated computer program developed by CRD to perform this function.

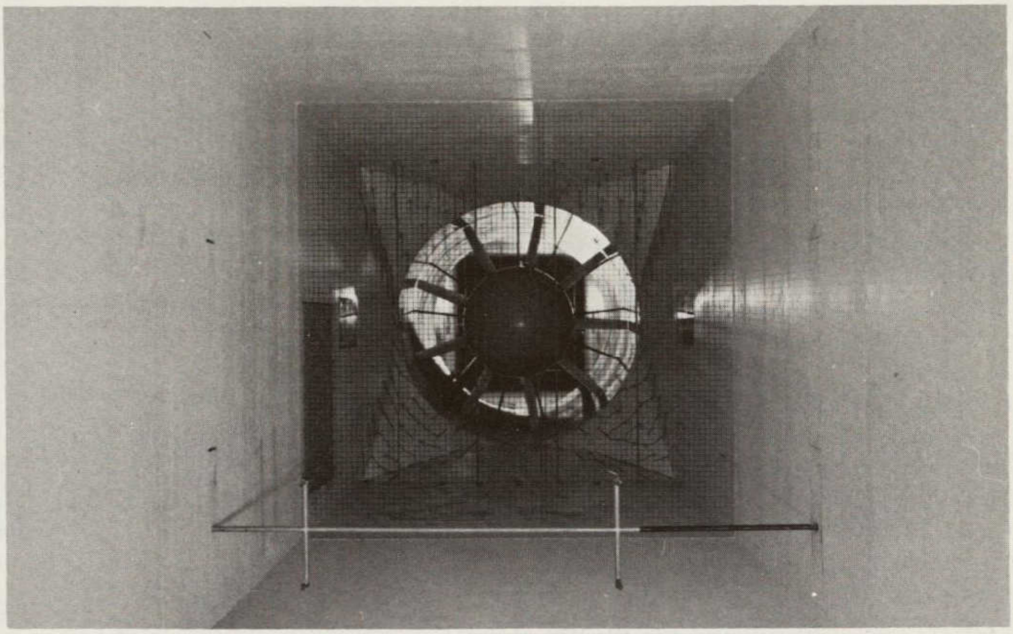

Figure 4. Microphone Probe in Station 3

1 (1) 1	2 (5) 1	3 (9) 1	4 (2) 2	5 (6) 2	6 (10) 2
7 (3) 3	8 (7) 3	9 (11) 3	10 (4) 4	11 (8) 4	12 (12) 4
13 (13) 1	14 (17) 1	15 (21) 1	16 (14) 2	17 (18) 2	18 (22) 2
19 (15) 3	20 (19) 3	21 (23) 3	22 (16) 4	23 (20) 4	24 (24) 4
25 (25) 1	26 (29) 1	27 (33) 1	28 (26) 2	29 (30) 2	30 (34) 2
31 (27) 3	32 (31) 3	33 (35) 3	34 (28) 4	35 (32) 4	36 (36) 4

Number	Meaning
Top	Cell Designation, Area No.
(Central)	Assumed Test Order (Record and Data Reduction)
Lower	Microphone No.

Figure 5. Microphone Positions in Duct Passage

Aerodynamic Performance Data-Reduction Computer Program

The computer program logic to evaluate fan performance is presented in Appendix B. It contains the equations and relationships that establish the fan adiabatic efficiency, corrected and normalized weight flow, and developed head conditions and fan input power based on the instrumentation system described in Appendix A.

The NASA standard sea-level temperature and pressure conditions of 518.7^{o}R and 14.69 psia were used as the reference base to which fan operating conditions were corrected. While this has merit when comparing fan performance to other NASA fans, it did require multiplying factors of 0.9786 and 0.978 to be applied to the reduced test data of corrected weight flow and developed head. These additional corrections were necessary because the original fan design was not based on NASA standard sea-level conditions but on estimated temperature and pressure values of 530^{o}F and 14.54 psia, thought to exist at the fan inlet of the 40 x 80 foot wind tunnel.

Acoustic Performance Data-Reduction Computer Program

The fan acoustic data reduction program developed by CRD, designated as "NASA FAN," is presented in Appendix C. The program is composed of six files: CONTROL, ATTENS, FANDATA, MIKEAREA, PAGE, and FANCALC. The exact function of each of these files is described as follows:

- CONTROL designates the actual order of data sampling.
- ATTENS lists record attenuator settings corresponding to the actual test order.
- FANDATA is the basic data file from the General Radio (GR) real-time analyzer.
- MIKEAREA is for microphone frequency response corrections, and cell areas expressed in decibels.
- PAGE is employed for paging of output data file.
- FANCALC is the output file for the reduced fan noise data.

A sample calculation is presented in Appendix C based on the cell designation and microphone positions presented in Figure 5. The frequency range of the output tabulations is automatically governed by control settings of the GR real-time analyzer. For fan-noise data reduction these will be set for 25 to 20,000 hertz, the available limits.

The actual sound-pressure spectra for the individual 36 samples are to be printed out so that it will be possible to evaluate the feasibility of reducing the number of sampling positions. In the sample calculation (Appendix C) the sound pressure levels (SPL's) are separated into three tabulations, with the double asterisks denoting the four corners of the three cell blocks.

Section 3

1/7-SCALE MODEL FAN EXPERIMENTAL PROGRAM AERODYNAMIC AND ACOUSTIC PERFORMANCE EVALUATION

As was pointed out in the introduction, the objective of the fan test program was to test two fan configurations, a high-speed and a low-speed fan, and determine which would be the quieter when scaled to full prototype fan size and speed. In addition, the quieter fan had to satisfy the tunnel head requirements at closed and open tunnel operating conditions.

From the outset it was recognized that achieving the fan design head and flow conditions would be more difficult with the low-speed fan than with the high-speed fan because of its higher hub loading. This hub loading condition would become even more aggravated if a hub/tip ratio of 0.4375 were to be employed in the final full-scale fan design than with the 0.5 hub/tip ratio employed in the first 1/7-scale model configuration.

Performance testing of the low-speed fan configuration would therefore be more involved than that of the high-speed fan. It would require several blade pitch settings to establish whether adequate design margin exists in meeting some of the more stringent, thickened-boundary-layer operating conditions than the tunnel corner fans would be subjected to.

In the case of the high-speed fan, with its lightly loaded blade conditions, a relatively short test program at design-pitch blade setting was thought to be adequate in establishing its capability in meeting its design performance objectives.

AERODYNAMIC PERFORMANCE OF HIGH-SPEED FAN

The aerodynamic performance of the high-speed fan at design stagger angle setting of 56° is shown in Figure 6. It can be seen that the fan meets its design head objective of 680 feet at the design corrected weight flow of 367 lb/sec, while its peak efficiency value of 86 percent at design flow is somewhat below the design efficiency value of 90 percent. Approximately 1-1/2 percent in efficiency loss can be attributed to the inlet-contraction section loss upstream of the fan, as evidenced by the total pressure survey at the fan inlet. (Overall fan performance based on surveys at stations 3 and 6 included the flowpath through the contraction section.)

A sample of the high-speed fan reduced performance data at design flow and speed based on the starboard azimuth-position radial survey at station 6 is shown in Figure 7. The radial total discharge pressure distributions for the four azimuth positions are in turn shown in plots of Figure 8. As can be seen from the plots of Figure 8, the blade-section radial performance patterns approach normality, with the usual decay in performance in the tip and hub regions caused by boundary layer effects.

ACOUSTIC PERFORMANCE OF HIGH-SPEED FAN

The acoustic performance data of intake exhaust and combined SPL spectra for both the 1/7-scale model fan and a cluster of six prototype fans are presented in Table 2 for the 100 percent design mass-flow condition. The variation of the dBA SPL spectra for the combined six prototype fans as a function of mass flow is presented in Figure 9. In arriving at the plots of Figure 9 and Table 2, the following scaling methods were employed.

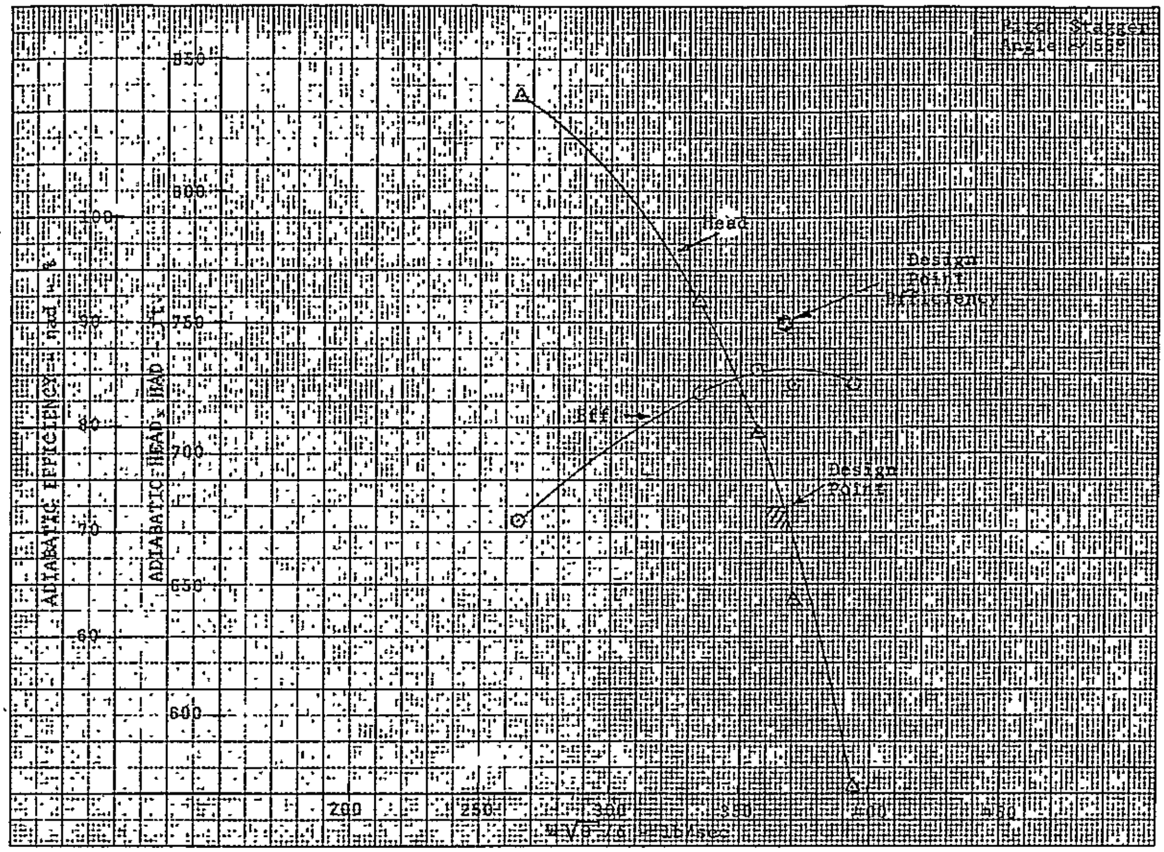

Figure 6. High-Speed Fan No. 1—Aerodynamic Performance

* * * * 1/7-SCALE 40 X 80 FAN MODEL PERFORMANCE * * * *

TEST 7-1-48, STATION 6, BLADE 56.08, THROTTLE 100.0, DESIGN SPEED 2000., SPEED CORRECTION FACTOR 1.00

RUN 12, STBD AZIMUTH PROBE INSTALLATION ANGLE ERRORS -- SWIRL -0.15, RADIAL -0.38

INPUT DATA, CONVERTED TO ENGINEERING UNITS --

PT	BAR. (IN HG)	T,H2O (DEG F)	T,INLET (DEG F)	PS,INLET (IWG)	PT,INLET (IWG)	T,DIS (DEG F)	PS,DIS (IWG)	PT,DIS (IWG)	SWIRL (DEG)	RADIAL (DEG)	R/RT	RPM	TORQ (FT LB)
1	30.22	89.24	48.05	-2.32	-0.49	51.57	-0.57	7.69	1.50	0.10	0.9884	1980.	1475.2
2							-0.63	9.08	1.69	0.15	0.9711		
3							-0.76	9.33	2.48	0.05	0.9514		
4							-0.75	9.97	3.62	0.02	0.9314		
5							-0.52	10.51	2.25	0.06	0.9109		
6							-0.52	11.14	2.22	-0.01	0.8899		
7							-0.47	11.75	2.31	-0.09	0.8685		
8							-0.67	11.87	3.69	-0.29	0.8465		
9							-0.56	12.05	4.19	-0.46	0.8239		
10	30.23	90.68	49.14	-2.32	-0.49	51.56	-0.57	12.01	4.64	-0.73	0.8006	1982.	1501.9
11							-0.67	11.96	5.64	-0.43	0.7767		
12							-0.67	11.89	6.07	-0.38	0.7520		
13							-0.72	11.56	6.71	-0.12	0.7264		
14							-0.72	11.53	6.64	-0.50	0.7000		
15							-0.70	11.35	6.24	-0.78	0.6725		
16							-0.72	11.04	6.27	-0.69	0.6439		
17							-0.75	10.45	5.55	-0.75	0.6138		
18							-0.77	9.46	4.30	-0.76	0.5823		
19							-0.70	8.84	1.46	-0.84	0.5490		
20	30.23	92.30	49.15	-2.32	-0.49	51.44	-0.59	7.06	0.74	-0.36	0.5135	1983.	1443.[illegible]

CALCULATED RUN RESULTS BASED ON 3 SAMPLES --

PT	PATM (PSIA)	TOA (DEG R)	PTOA (PSIA)	TOR (DEG R)	PTOJ (PSIA)	WSUM (LB/SEC)	WR (LB/S)	WCOR (LB/S)	WNOR (LB/S)	PR	HISNOR (FEET)	HPINP (HP)	ETA
1	14.84	507.6	14.83	511.2	15.2.	365.4	366.5	359.3	363.0	1.0270	723.8	556.14	0.869
10	14.85	507.7	14.83	511.2	15.23	365.4	367.0	359.8	363.1	1.0270	721.3	566.77	0.852
20	14.85	507.6	14.83	511.0	15.23	365.4	366.5	359.6	362.7	1.0270	721.4	563.91	0.857

Figure 7. High-Speed Fan—Reduced Performance Data

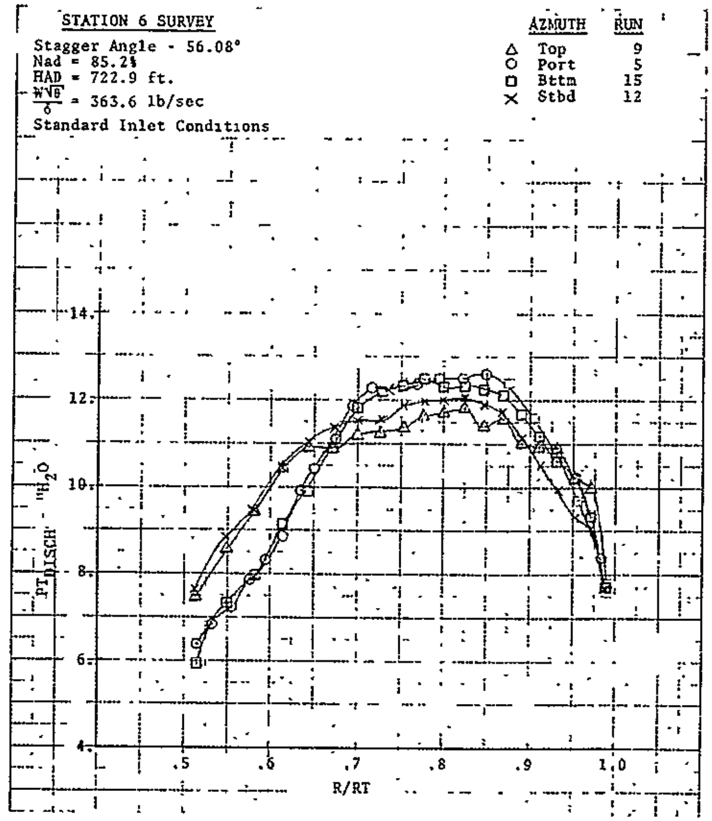

Figure 8. High-Speed Fan—Radial Discharge Total Pressure Distribution At Design Flow

The 1/3-octave-band noise levels of the model fan were first converted to prototype (6 fans) noise levels by applying the simple fan-noise-scaling-low relationship of

$$\text{dB}\begin{pmatrix}\text{Prototype}\\ \text{6 Fans}\end{pmatrix} = \text{dB (model)} + 10 \log_{10}\left[\frac{6 \times \text{W prototype}}{\text{W Model}}\right]$$

The frequencies were then shifted by the 0.15-scale factor of the model fan diameter to full-scale fan diameter; and lastly, the dBA weighting factor was applied to the shifted 1/3-octave-band frequency noise levels in arriving at the dBA sound power levels for the Prototype (6 fans).

The total sound power levels for the 1/7-scale model high-speed fan and the six prototype fans were respectively 127.8 dBA and 146.8 dBA. These compared to predicted values of 136.8 dBA and 152.5 dBA respectively for the high-speed fan model and the six prototype fans. While deviation between predicted and tested noise levels for the high-speed prototype fans of 5.7 dBA was appreciable, the predicted noise level for the low-speed fans of 139.4 dBA was still 7.4 dBA below that of the indicated noise level of the high-speed fan. The potential gain of employing low-speed fans was therefore still appreciable, and the test program as originally outlined was continued.

AERODYNAMIC PERFORMANCE OF LOW-SPEED FAN

The aerodynamic performance testing program on the lowspeed fan was contingent on verification of the acoustic advantage of the low-speed fan over that of

Table 2

HIGH-SPEED FAN--NOISE SPECTRA AT DESIGN SPEED AND FLOW

HIGH SPEED FAN 100% MASS FLOW

FREQUENCY	INTAKE LW RE 1E-12 WATTS		EXHAUST LW RE 1E-12 WATTS		TOTAL LW RE 1E-12 WATTS	
HERTZ	MODEL	PROTOTYPE (SIX FANS)	MODEL	PROTOTYPE (SIX FANS)	MODEL	PROTOTYPE (SIX FANS)
25	107.50	128.71	117.04	139.50	117.50	139.85
31	105.28	129.64	118.02	138.34	118.25	138.89
40	104.47	134.06	118.11	138.96	118.29	140.18
50	104.25	144.03	117.64	146.85	117.83	148.68
63	104.56	133.13	117.37	136.43	117.59	138.10
80	104.48	134.22	117.90	137.10	118.09	138.90
100	105.18	140.81	116.74	144.48	117.03	146.03
125	104.94	135.16	115.99	136.97	116.32	139.17
160	104.45	136.72	115.24	138.54	115.59	140.73
200	105.38	136.82	114.08	138.65	114.63	140.84
250	109.80	135.99	114.70	137.78	115.92	139.99
315	119.77	136.02	122.59	136.59	124.42	139.32
400	108.87	135.70	112.17	135.79	113.84	138.76
500	109.96	135.36	112.85	135.52	114.65	138.45
630	116.55	135.60	120.22	135.39	121.77	138.51
800	110.90	135.94	112.71	135.80	114.91	138.88
1000	112.46	135.56	114.28	135.26	116.47	138.42
1250	112.56	134.86	114.39	134.43	116.58	137.66
1600	111.73	133.58	113.52	133.13	115.73	136.37
2000	111.76	131.63	112.33	131.49	115.06	134.57
2500	111.44	128.28	111.53	128.31	114.50	131.31
3150	111.10	125.99	111.26	127.09	114.19	129.59
4000	111.34		111.13		114.25	
5000	111.68		111.54		114.62	
6300	111.30		111.00		114.16	
8000	110.60		110.17		113.40	
10000	109.32		108.87		112.11	
12500	107.37		107.23		110.31	
16000	104.02		104.05		107.05	
20000	101.73		102.83		105.53	
DBA	123.90	143.82	125.48	143.84	127.77	146.84

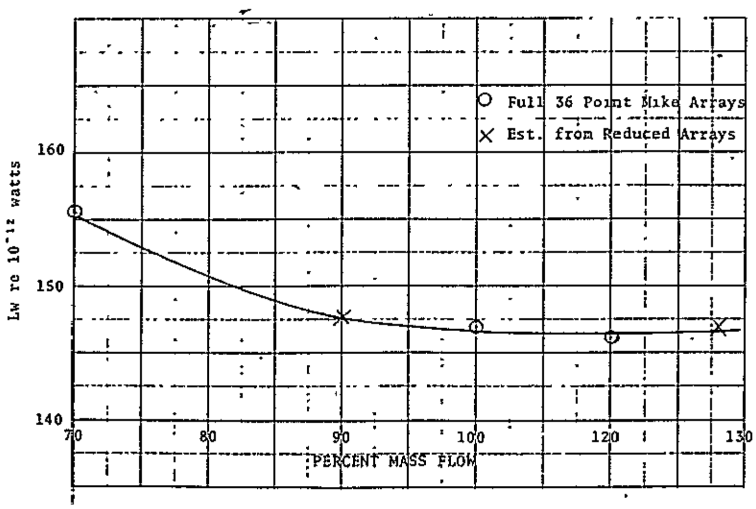

Figure 9. Sound Power Levels with Mass Flow for High-Speed Fans

the high-speed fan. The initial tests were made on the low-speed fan (specific details are discussed below under "Acoustic Performance of Low-Speed Fan"), and the planned comprehensive low-speed aerodynamic fan test program was then carried out.

A total of 487 test runs were completed on low-speed fan configuration No. 1, whereas only 23 test runs were made on the high-speed fan. The complete summary of the tests conducted on both the high-speed and low-speed fans is presented in Appendix D.

Aerodynamic Performance Deficiency

The initial tests of the low-speed fan at the design stagger-angle setting of 40.8° showed a serious deficiency in performance. This was the result of poorer fan efficiency (82% vs a design efficiency of 90%) and insufficient work addition imparted by the blades to the air. While the lower work input at a stagger angle of 40.8° could be corrected by operating the fan at a higher angle of attack or a reduced stagger angle setting, improvement in fan efficiency would require modification of the fan blade shapes.

Unlike the high-speed fan performance characteristic, the low-speed fan exhibited a sensitivity to azimuth position that appeared to be associated with inlet flow distortion. The test results showed that at the 100 percent flow and speed setting for the 40.8° stagger angle setting a deviation of 10 percent in developed head existed between the port azimuth total pressure survey and the starboard total pressure survey, or 536 feet versus 485 feet respectively. The port azimuth measuring station is in a line of sight of undisturbed inlet bellmouth flow, while on the starboard side of the bellmouth the flow is disturbed by the wall forward and along the side of the inlet (Figure 2).

Aerodynamic Performance Testing with Honeycomb Section Upstream of Fan

In order to reduce the flow distortion produced by the ground and sidewall effects at the inlet to the test vehicle bellmouth section, a honeycomb section was introduced in the vicinity of the inlet distortion screen designated as Station 18'-3" in the schematic of Figure 3. The low-speed fan tests were then repeated with the design stagger angle setting of 40.8° and with stagger angle settings of 38° and 35.4°. The performance results of these tests are presented in Figure 10. While a small improvement in performance in the order of 3 to 4 percent increase in weight flow was achieved with the honeycomb section for the design stagger angle setting of 40.8°, it was relatively insignificant compared with the large effect in developed head produced by small changes in blade stagger angle setting.

Effect of Rotor-Blade Stagger Angle on Fan Performance

As can be seen from Figure 10, the rotor-blade stagger angle setting of 38° achieved the highest fan efficiency of 83 percent, but at a reduced developed head of 94 percent of design head. This particular test did have the benefit of a less severe annulus passage contraction upstream of the fan. In terms of good stall margin and reasonable radial profiles, the 38° stagger angle setting appeared to be the most favorable. The radial total pressure profiles for this stagger angle setting shown in Figure 11, with the exception of the starboard profile, exhibit a nearly normal radial distribution, with a greater performance decay towards the hub region than the tip

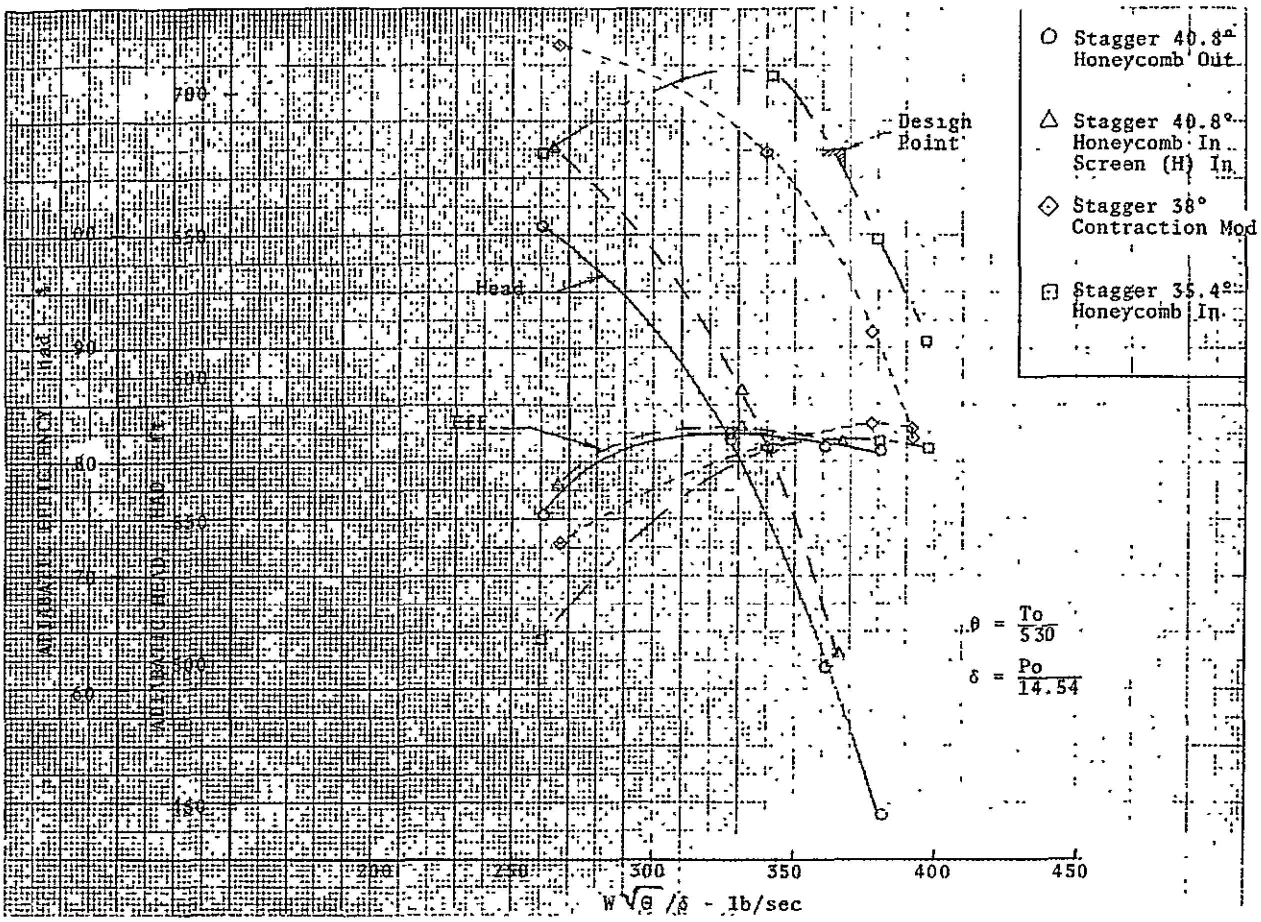

Figure 10. Low-Speed Fan No. 1—Aerodynamic Performance

region. Again both the starboard and bottom azimuth total pressure profiles are the weakest, with the starboard profile exhibiting serious performance deterioration over nearly 40 percent of its blade height. This sensitivity of fan performance deterioration to inlet flow distortion could put a serious limitation on the original fan blade design in its ability to meet the more severe boundary layer effects that exist at the inlet of the full-scale fans of the 40x80 foot wind tunnel.

Of the various low-speed fan blade angle settings, the 35.4° stagger angle did approach achieving the design head of 680 feet. It showed, however, a limited flow range capability, with stalling characteristics appearing at the 90 percent flow condition. Based on the above test results and factoring in the more stringent performance requirements contemplated for the full-scale fans—(1) operating with a reduced fan hub/tip ratio of 0.4375, and (2) with significantly thickened inlet boundary layers generated by the tunnel walls—the original aerodynamic design of the low-speed fan became questionable in its ability to meet the full-scale fan performance objectives of the 40x80 foot wind tunnel.

ACOUSTIC PERFORMANCE OF LOW-SPEED FAN

The acoustic test results for the low-speed fan are presented in Tables 3, 4, and 5. Table 5 shows the low-speed-fan noise frequency spectra for the model and six prototype fans corresponding to the design-developed head and flow condition of the fan. Tables 3 and 4 are summaries of the reduced acoustic results for the low-speed fan generated by CRD.

Table 3

NASA-AMES LOW SPEED FAN MODEL NOISE TESTS - DBA SOUND POWER LEVEL SUMMARY

RUN NO.	31	[illegible]	31/23	70	70	70	70	70	70	70
STAGGER ANGLE	40.8	40.8	40.8	35.4	35.4	35.4	35.4	35.4	35.4	35.4
% SPEED	100	100	100	100	100	100	100	100	90	90
% MASS FLOW	70	90	100	70	90	100	105	110	80	100
MODEL dBA L_W										
Intake	120.8	120.5	119.7	123.2	122.2	122.4	122.6	122.7	119.6	119.5
Exhaust	122.1	122.3	122.4	124.0	123.6	124.5	124.7	124.7	120.7	122.0
Total	124.5	124.5	124.3	126.6	126.0	126.6	126.8	126.6	123.2	123.9
PROTOTYPE dBA L_W (six fans)										
Intake	138.2	138.1	135.9	140.5	140.0	139.6	139.4	138.9	136.9	135.9
Exhaust	139.3	139.0	138.7	140.3	140.8	141.1	141.2	141.3	137.4	138.1
Total	141.3	141.6	140.5	143.4	143.4	143.4	143.4	143.4	140.2	140.1
TAPE REEL NO.	3	3	3	7	7	7	7	7	7	7

RUN NO.	135	135	135	135	135	171	171	171	171
STAGGER ANGLE	45.2	45.2	45.2	45.2	45.2	35.4	35.4	35.4	35.4
% SPEED	100	100	100	100	70	100	100	100	100
% MASS FLOW	70	80	100	110	100	70	90	100	105
MODEL dBA L_W									
Intake	122.0	119.8	116.9	116.6	105.9	123.3	120.3	121.0	120.6
Exhaust	124.0	121.8	119.6	119.6	109.8	126.9	124.8	125.1	124.6
Total	126.1	123.9	121.7	121.4	111.6	128.5	126.1	126.5	126.1
PROTOTYPE dBA L_W (six fans)									
Intake	138.7	137.3	133.9	133.1	123.1	138.3	136.8	136.6	136.8
Exhaust	140.8	139.3	136.6	135.2	125.4	142.8	142.2	141.8	141.5
Total	142.9	141.4	138.5	137.3	127.4	144.1	143.3	142.9	142.8
TAPE REEL NO.	9	9	9	9	9	10	10	10	10

RUN NO.	210	210	210	210	290	290	290
STAGGER ANGLE	52.8	52.8	52.8	52.8	40.8	40.6	40.8
% SPEED	100	100	100	100	100	100	100
% MASS FLOW	70	90	100	105	70	90	100
MODEL dBA L_W							
Intake	125.2	114.9	112.2	112.0	119.7	119.8	119.2
Exhaust	128.3	118.5	116.4	115.5	123.5	123.0	122.1
Total	130.4	120.1	117.8	117.1	125.0	124.7	123.9
PROTOTYPE dBA L_W (six fans)							
Intake	137.0	130.6	128.4	128.3	135.8	135.5	135.1
Exhaust	142.1	135.7	132.9	131.1	140.6	139.6	138.7
Total	143.3	136.9	134.2	132.9	141.8	141.0	140.3
TAPE REEL NO.	11	11	11	11	12	12	12

Table 4

NASA-AMES LOW SPEED FAN MODEL NOISE TESTS - DBA SOUND POWER LEVEL SUMMARY

RUN NO.	231	231	231	327	327	327	327	327	328	328	328	338	338	338
STAGGER ANGLE	40.8	40.8	40.8	88.4	88.4	88.4	88.4	88.4	62.9	62.9	62.9	62.9	62.9	62.9
% SPEED	100	100	100	50	75	80	90	100	100	100	100	100	100	100
% MASS FLOW	75	95	105	100	100	100	100	100	90	100	120	90	100	110
MODEL dBA L_w														
Intake	120.9	[illegible]	118.7	94.2	104.7	106.1	109.5	111.6	124.2	124.6	119.7	124.8	125.2	119.9
Exhaust	[illegible]	[illegible]	122.3	94.8	105.0	106.2	109.6	112.1	127.4	127.5	123.0	127.4	127.7	122.9
Total	125.2	124.5	123.9	97.5	107.9	109.2	112.6	114.9	129.1	129.3	124.7	129.3	129.6	124.7
PROTOTYPE dBA L_w (six fans)														
Intake	[illegible]	[illegible]	134.4	107.3	118.1	119.7	123.3	125.9	135.7	136.2	134.5	136.3	136.9	134.9
Exhaust	[illegible]	[illegible]	139.7	[illegible]	118.9	120.5	124.0	126.8	139.8	140.2	138.5	140.1	140.7	138.7
Total	[illegible]	141.0	140.1	110.8	121.5	123.1	126.7	129.4	141.2	141.7	140.0	141.6	142.2	140.2
TAPE REEL NO	13	13	13	14	14	14	14	14	14	14	14	15	15	15

RUN NO.	465	466	466	466	466	496	496	496	496	495	496	496
STAGGER ANGLE	40.8	40.8	40.8	40.8	40.8	38	38	38	39	38	[illegible]	[illegible]
% SPEED	100	100	90	75	50	100	100	100	90	80	75	50
% MASS FLOW	100	100	100	100	100	105	100	90	100	100	100	100
MODEL dBA L_w												
Intake	126.3	124.0	120.2	116.5	106.6	125.3	125.3	126.1	122.6	119.5	115.7	107.8
Exhaust	130.5	126.2	122.6	117.4	107.7	128.4	129.6	129.3	125.6	121.6	119.7	[illegible]
Total	131.9	128.2	124.6	120.0	110.2	130.1	131.0	131.0	127.4	125.2	121.5	111.2
PROTOTYPE dBA L_w (six fans)												
Intake	139.0	137.1	133.5	128.6	118.5	138.8	138.7	138.8	135.1	132.3	129.4	119.5
Exhaust	144.1	140.2	136.8	131.5	120.2	142.2	142.8	143.4	138.8	135.4	133.3	121.7
Total	145.3	141.9	138.5	133.3	122.4	143.8	144.2	144.7	140.3	138.3	134.8	123.7
TAPE REEL NO	16	17	17	17	17	18	18	18	18	18	18	18

Table 5

LOW-SPEED FAN--NOISE SPECTRA
AT DESIGN SPEED AND FLOW

LOW SPEED FAN 35.4 DEGR. 100% SPEED 100% FLOW

FREQUENCY HERTZ	LW RE 1E-12 WATTS MODEL	PROTOTYPE (SIX FANS)
25	122.9	142.8
31	122.6	142.1
40	122.6	142.1
50	121.6	142.7
63	121.1	140.8
80	120.7	141.2
100	119.9	145.2
125	119.4	140.6
160	118.5	140.6
200	117.8	141.1
250	117.8	139.2
315	118.5	137.5
400	116.6	137.5
500	117.0	136.3
630	121.0	135.2
800	116.3	133.9
1000	116.3	132.4
1250	116.8	132.0
1600	115.0	130.4
2000	113.2	127.8
2500	113.3	124.4
3150	112.0	125.5
4000	110.9	
5000	109.7	
6300	108.2	
8000	107.8	
10000	106.2	
12500	103.5	
16000	100.2	
20000	101.2	
DBA	126.5	142.9

As was previously described in Figure 10, the low-speed fan has to operate at the reduced stagger angle setting of 35.4° to attain design-developed head. This somewhat penalized its acoustic performance. The noise levels for the low-speed fan at design operating conditions are respectively 126.5 and 142.9 dBA for the model and six prototype fans. This falls short of the originally predicted noise levels of 122.1 and 139 dBA respectively for the model and six prototype fans. Yet, in spite of this deficiency in realizing the predicted noise levels for the low-speed fan, the test results showed a definite significant reduction in fan noise generation in going to the low-speed configuration.

Comparison of Acoustic Performance of Low-Speed and High-Speed Fan Configurations

The low-speed fan noise test results at design operating conditions (Table 4, Run 171) are 126.5 and 142.9 dBA respectively for the model and six prototype fans. This compares to noise levels for the high-speed fan configurations of 127.7 and 146.8 dBA. While this comparison shows a net reduction in the order of 4 dBA in going from the high-speed to the low-speed fan configuration, it represents a conservative comparison.

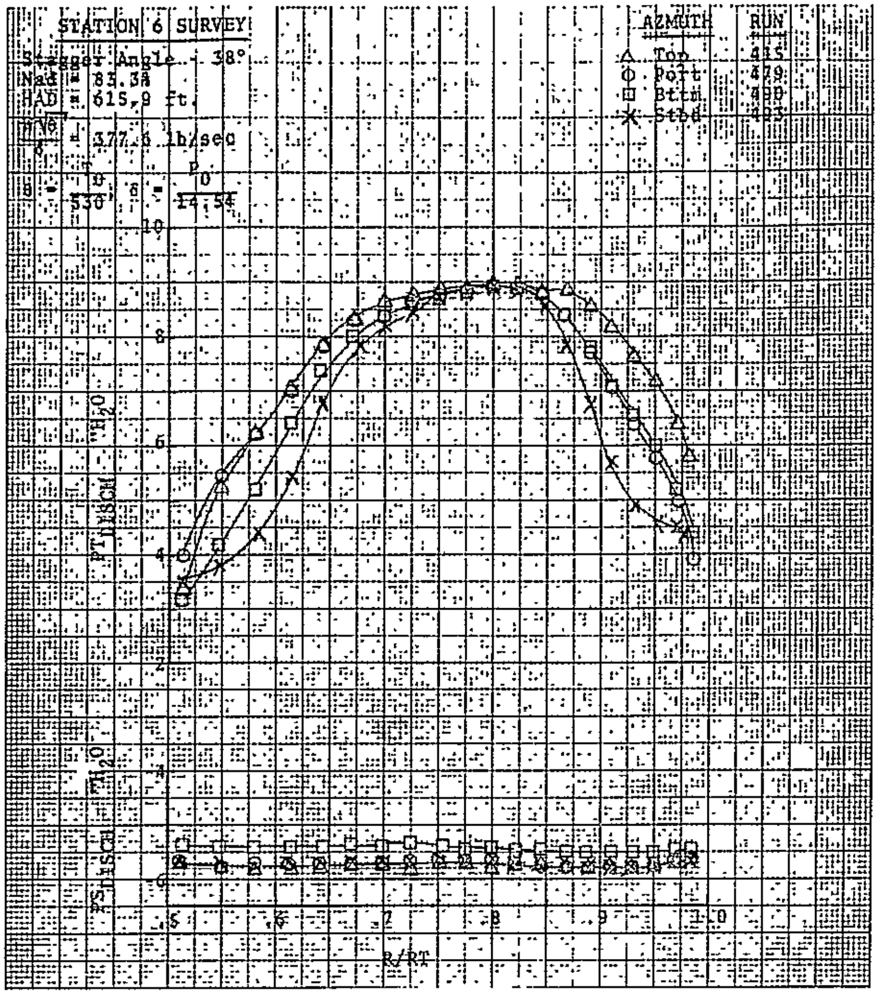

Figure 11. Low-Speed Fan—Radial Discharge Total Pressure Distribution

As the noise comparisons for the low-speed and high-speed fans were made at design head and flow, this somewhat penalized the low-speed noise operation. In order to meet design head, the low-speed fan with its deficiency in both turning and efficiency had to be operated at a 5° blade incidence setting, or a less favorable incidence condition from the standpoint of noise generation than that of the high-speed fan. Comparing the two fan configurations at their design incidence conditions, corresponding to a stagger angle setting of 40.8° for the low-speed fan, a further reduction in noise level is realized by the low-speed fan. Run No. 291 in Table 5, corresponding to the low-speed fan's stagger angle setting of 40.8°, shows a noise level for the prototype six fans of 140.1 dBA. This represents a noise reduction of 6.7 dBA in going from the high-speed to the low-speed fan configuration. Based on the above analysis, it would appear reasonable to project that with an improved low-speed fan design it would be possible to achieve a noise level reduction with the low-speed fan that would be midway between the two test comparisons of Runs 171 and 291. This would represent a noise reduction of 5.3 dBA for the low-speed fan over that of the high-speed fan.

AERODYNAMIC PERFORMANCE OF LOW-SPEED FAN WITH ARTIFICIALLY GENERATED INLET DISTORTIONS

The inlet flow distortions that were introduced at the fan entrance are shown in Figure 12. The obstructions that were introduced at the inlet to the model fan were designed to simulate the thickened boundary layer conditions on the tunnel walls upstream of the six-fan cluster.

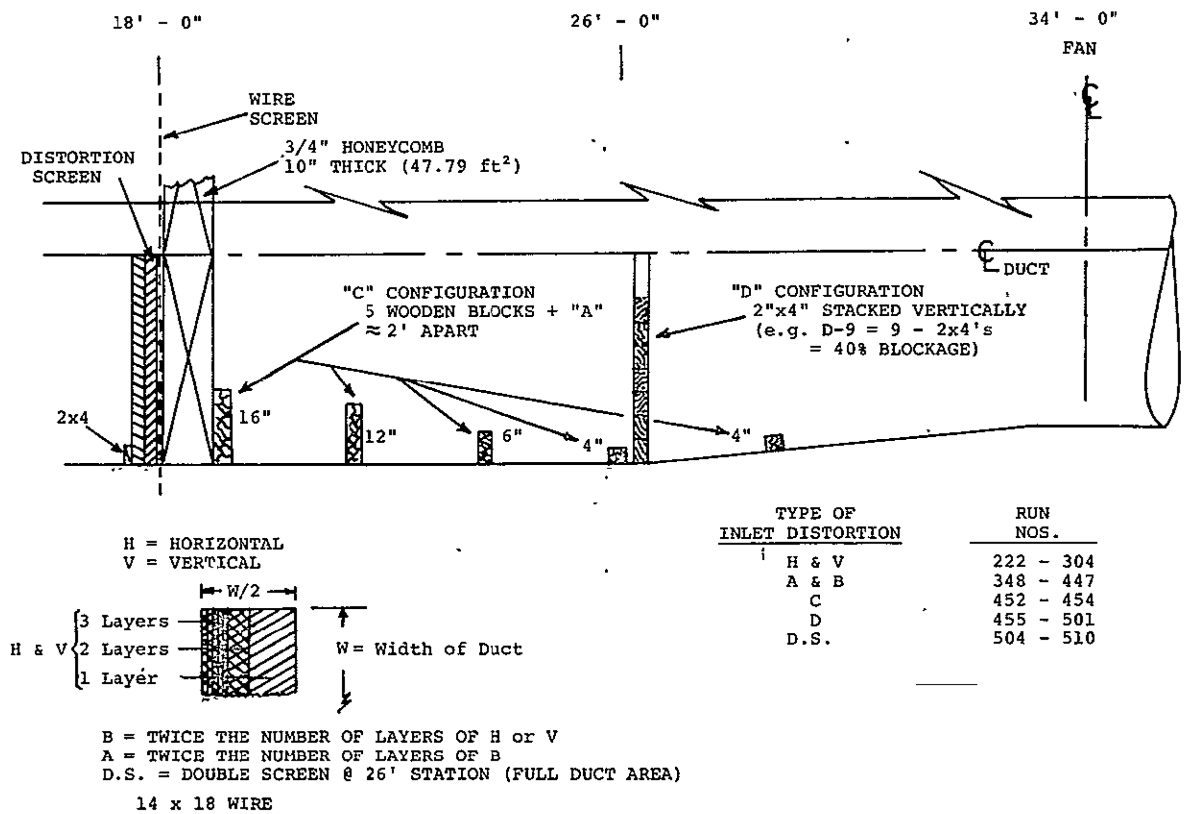

TYPE OF INLET DISTORTION	RUN NOS.
H & V	222 - 304
A & B	348 - 447
C	452 - 454
D	455 - 501
D.S.	504 - 510

Figure 12. Low-Speed Fan — Inlet Distortions

Based on the test results it appears that the fan tip section is able to operate with a highly distorted flow without stalling. This is illustrated by the test results with maximum blockage, corresponding to configuration D-9 (Figure 12). Examination of computer output sheets for the inlet and discharge fan performance, presented in Figures 13 and 14 for Runs 461 and 462 corresponding to the bottom azimuth surveys at stations 4 and 6 respectively, shows that with a severely skewed velocity profile from tip to hub, the tip section had no problem in exceeding design-developed head by approximately 20 percent. Furthermore, the developed head rise of 821 feet for the entire radial blade section, based on the total pressure rise data from the station 4 to 6 survey probe; seems to indicate the ability of the fan to operate with a thickened boundary layer over a circumferential sector without stalling. The data, however, are not conclusive, since only two of the four azimuth positions (bottom and top) were surveyed. There is conceivably a circumferential shift of the poor-performance regions of the fan that would have shown up in either the port or starboard survey position had they been taken, and the overall fan performance may actually be poorer than that indicated by the more favorable results shown by the bottom and top azimuth surveys.

ORIGINAL PAGE IS OF POOR QUALITY

TEST 7-2-48 * * * * 1/7-SCALE 40X80 FAN MODEL PERFORMANCE * * * * (UPDATE 8/ 5/75)

FAN STAGGER ANGLE 40.80, SURVEY STATION 4, THROTTLE 100.0 PCT, FAN DESIGN SPEED 1200. RPM, SPEED CORR. FACTOR 1.00

RUN 461, (BTTM AZIMUTH) PROBE INSTALLATION ANGLE ERRORS -- SWIRL 1.26 DEG, RADIAL 0.10 DEG

INPUT DATA, USING STATION ** 1 ** INLET STATIC PRESSURE, CONVERTED TO ENGINEERING UNITS --

PT	BAR. (IN HG)	T,H2O (DEG F)	T,INLET (DEG F)	PS,INLET (1)(IWG)	PT,INLET (3)(IWG)	T,DIS (DEG F)	PSC,DIS (IWG)	PTC,DIS (IWG)	SWIRL (DEG)	RADIAL (DEG)	R/RT	RPM	TORK (FT LB)
1	29.93	82.22	58.68	-1.90	-3.51	60.79	-13.55	-11.64	-2.19	-1.34	0.9882	1197.	1980.3
2							-14.01	-12.00	-1.33	0.05	0.9711		
3							-14.55	-12.43	2.03	1.60	0.9514		
4							-14.91	-12.66	2.31	4.89	0.9315		
5							-15.11	-12.87	0.42	3.21	0.9110		
6							-15.44	-13.05	-0.29	3.73	0.8902		
7							-15.77	-13.21	-2.06	5.12	0.8685		
8							-15.42	-12.60	0.37	7.49	0.8465		
9							-15.47	-12.19	-0.57	7.94	0.8240		
10	29.93	82.40	57.98	-1.90	-3.55	61.28	-15.63	-12.45	-0.70	6.69	0.8007	1196.	1982.0
11							-15.73	-11.85	-0.66	7.12	0.7766		
12							-15.54	-10.89	-0.75	8.46	0.7521		
13							-15.44	-10.35	-0.03	9.55	0.7265		
14							-15.28	-9.77	0.04	8.45	0.7001		
15							-15.22	-9.12	0.70	7.89	0.6726		
16							-15.23	-8.65	0.91	7.20	0.6439		
17							-14.95	-7.61	1.01	6.83	0.6140		
18							-14.88	-7.03	0.71	5.55	0.5824		
19							-14.68	-6.02	1.89	4.35	0.5490		
20	29.93	82.40	57.78	-1.92	-3.59	61.23	-14.16	-5.60	2.02	2.69	0.5134	1194.	1973.6

CALCULATED RUN RESULTS BASED ON 3 SAMPLES AND PRODUCED WITH 3 ERROR WARNINGS --

PT	PATM (PSIA)	TOA (DEG R)	PTOA (PSIA)	TDR (DEG R)	PTDJ (PSIA)	WSUM (LB/SEC)	WN (LB/S)	WCOR (LB/S)	WNOR (LB/S)	PR	HISNOR (FEET)	HPINP (HP)	ETA
1	14.70	518.3	14.57	520.4	14.33	212.8	327.1	329.7	330.5	0.9834	-464.2	451.33	-0.609
10	14.70	517.6	14.57	520.9	14.33	212.7	327.5	329.9	331.0	0.9835	-460.8	451.33	-0.605
20	14.70	517.4	14.57	520.8	14.33	212.8	329.4	331.7	333.4	0.9836	-459.4	448.69	-0.608
AVG	14.70	517.7	14.57	520.7	14.33	212.3	328.0	330.5	331.7	0.9835	-461.5	450.44	-0.608

Figure 13. Low-Speed Fan—Inlet Survey with Inlet Obstructions; Station 4

TEST 7-2-48 * * * * 1/7-SCALE 40X80 FAN MODEL PERFORMANCE * * * * (UPDATE 8/ 5/75)

FAN STAGGER ANGLE 40.80, SURVEY STATION 6, THROTTLE 100.0 PCT, FAN DESIGN SPEED 1200. RPM, SPEED CORR. FACTOR 1.00

RUN 462, (BTTM AZIMUTH) PROBE INSTALLATION ANGLE ERRORS -- SWIRL -0.63 DEG, RADIAL -0.25 DEG

INPUT DATA, USING STATION ** 1 ** INLET STATIC PRESSURE, CONVERTED TO ENGINEERING UNITS --

PT	BAR. (IN HG)	T,H2O (DEG F)	T,INLET (DEG F)	PS,INLET (1)(IWG)	PT,INLET (3)(IWG)	T,DIS (DEG F)	PSC,DIS (IWG)	PTC,DIS (IWG)	SWIRL (DEG)	RADIAL (DEG)	R/RT	RPM	TORK (FT LB)
1	29.94	81.63	59.11	-1.92	-3.59	62.44	-4.34	1.55	10.56	1.19	0.9895	1195.	1999.3
2							-4.36	2.32	10.54	1.15	0.9712		
3							-4.32	2.70	10.90	1.34	0.9516		
4							-4.47	2.78	10.97	1.51	0.9315		
5							-4.52	2.38	10.40	1.59	0.9109		
6							-4.55	2.88	9.95	1.79	0.8900		
7							-4.57	2.76	9.11	1.74	0.8695		
8							-4.59	2.70	8.47	1.95	0.8465		
9							-4.63	2.44	7.78	2.04	0.8240		
10	29.94	81.86	59.09	-1.88	-3.56	62.12	-4.67	2.18	6.93	2.20	0.8007	1196.	1978.6
11							-4.61	2.08	6.31	2.09	0.7766		
12							-4.67	1.62	6.02	2.16	0.7520		
13							-4.59	1.32	5.33	2.02	0.7265		
14							-4.61	0.82	5.22	2.12	0.7002		
15							-4.57	0.50	5.09	1.78	0.6726		
16							-4.61	0.13	4.74	1.63	0.6439		
17							-4.59	-0.19	4.14	1.29	0.6140		
18							-4.59	-0.49	2.50	1.05	0.5825		
19							-4.56	-0.49	-0.89	0.70	0.5491		
20	29.94	81.50	59.14	-1.96	-3.64	62.29	-4.46	-0.49	-4.26	0.12	0.5134	1196.	1987.0

CALCULATED RUN RESULTS BASED ON 3 SAMPLES AND PRODUCED WITH 3 ERROR WARNINGS --

PT	PATM (PSIA)	TOA (DEG R)	PTOA (PSIA)	TDR (DEG R)	PTDJ (PSIA)	WSUM (LB/SEC)	WN (LB/S)	WCOR (LB/S)	WNOR (LB/S)	PR	HISNOR (FEET)	HPINP (HP)	ETA
1	14.71	518.7	14.58	522.0	14.76	259.6	329.8	331.5	332.9	1.0125	348.5	452.85	0.456
10	14.71	518.6	14.58	521.7	14.76	259.7	325.4	328.0	329.1	1.0125	345.8	450.57	0.451
20	14.71	518.7	14.57	521.9	14.76	259.7	332.3	335.0	336.2	1.0127	351.1	452.47	0.466
AVG	14.71	518.7	14.58	521.9	14.76	259.7	328.8	331.5	332.7	1.0126	348.5	451.96	0.458

Figure 14. Low-Speed Fan—Discharge Survey with Inlet Obstructions; Station 6

It would appear, therefore, that the inlet distortion tests on the low-speed fan should be repeated with survey data taken at the four azimuth positions, to more correctly ascertain how well the 40-foot-diameter fans will perform in the presence of a distorted flow due to a thickened boundary layer.

PRECEDING PAGE BLANK NOT FILMED

Section 4

RESTUDY OF LOW-SPEED FAN REDESIGN

The aerodynamic test results on the low-speed fan established that the fan hub profile was poor and would further deteriorate in going from a hub/tip ratio of 0.5 to 0.4375. It was, therefore, decided to reevaluate the fan blade design procedures in arriving at the original rotor and stator blade shapes for the low-speed fan. In order to capitalize on the advanced analytical procedures for fans that are available within the General Electric Company, this study phase was turned over to GE's Aircraft Engine Business Group's Advanced Turbomachinery Aeodynamics Subsection under the direction of Dr. Leroy H. Smith, Jr.

RESULTS AND RECOMMENDATIONS OF LOW-SPEED FAN AERODYNAMIC STUDY BY GE'S AIRCRAFT ENGINE BUSINESS GROUP (AEBG)

The aerodynamic fan study evaluated the following rotor and stator blade design areas:

- Rotor and stator blade chord length distribution with radius.
- Rotor and stator airfoil maximum thickness ratio with radius.
- Rotor and stator camber angle distribution with radius.
- Rotor and stator stagger angle distribution with radius.
- Basic airfoil thickness distribution for the rotor and stator and blade stacking arrangement.

Rotor and Stator Blade Geometry Recommendations

The recommended rotor and stator blade geometry modifications resulting from the aerodynamic study are shown in Figures 15 through 20.

Blade Chord Length and Thickness Distribution

Changes in the stator chord length and rotor and stator blade thickness distribution are shown in Figures 15 and 16. All of these values were increased from the original design. The increase in stator chord length was incorporated to improve its stall resistance; the increase in blade thickness distribution was mainly dictated by structural considerations.

Blade Camber

The blade camber shape shown in Figure 17 was considerably modified from its original design for both the rotor and stator. The curlups in camber at the hub are primarily a result of the recognition of end-wall boundary layer effects that show up as increased losses and a consequent requirement for increased air deflection there. At the tip the camber curlups are also partly due to increased losses, but an additional consideration adds to the camber. This is the assumption of a slightly reduced inlet total pressure toward the tip in anticipation that the inlet profile, treated on a circumferential-average basis, will be better matched this way. The magnitude of this assumed inlet total-pressure distortion is small. It represents a 10 percent lower-tip

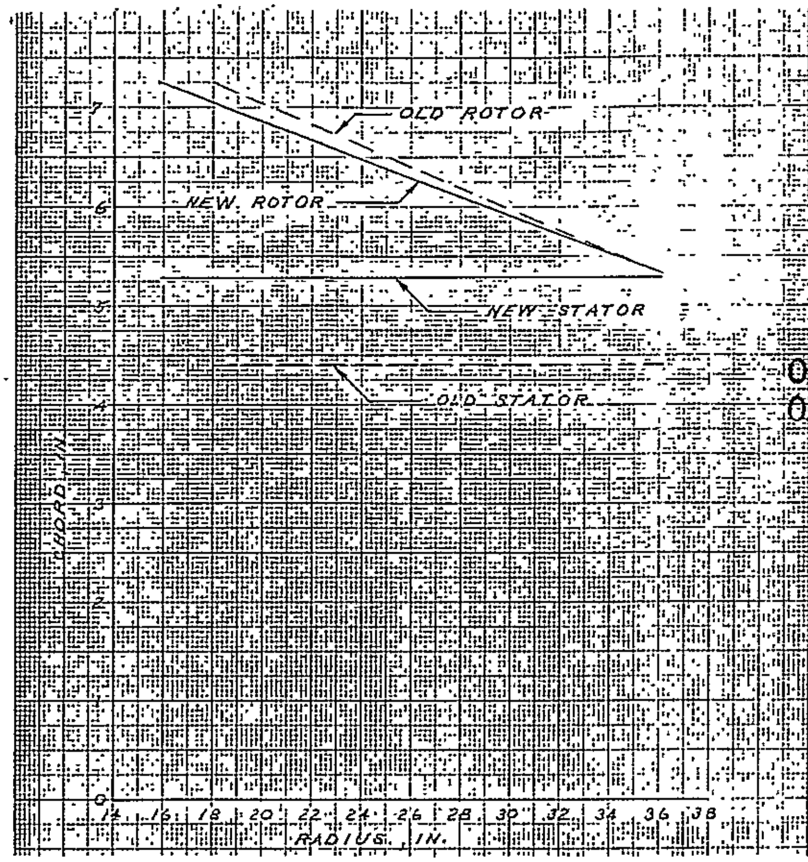

Figure 15. Blade Channel Length vs Radius

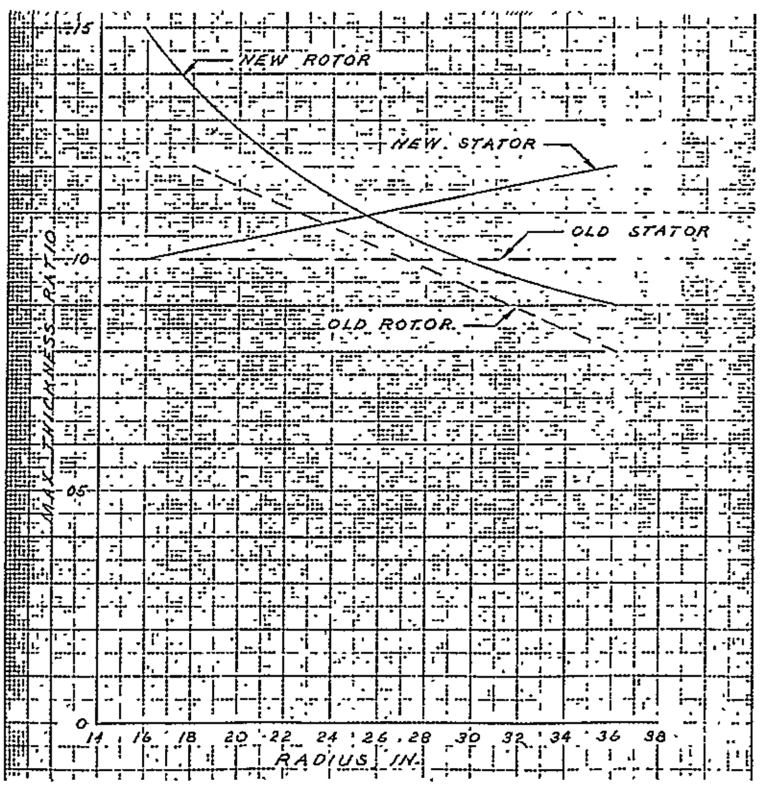

Figure 16. Maximum Thickness Ratio vs Radius

axial velocity than the hub axial velocity when calculated under the assumption that the static pressure is uniform. With the nonuniform static pressure that was actually computed to exist at the rotor face, the axial velocity distribution from tip to hub was not so severe, the tip having an axial velocity only 4 percent lower than the hub.

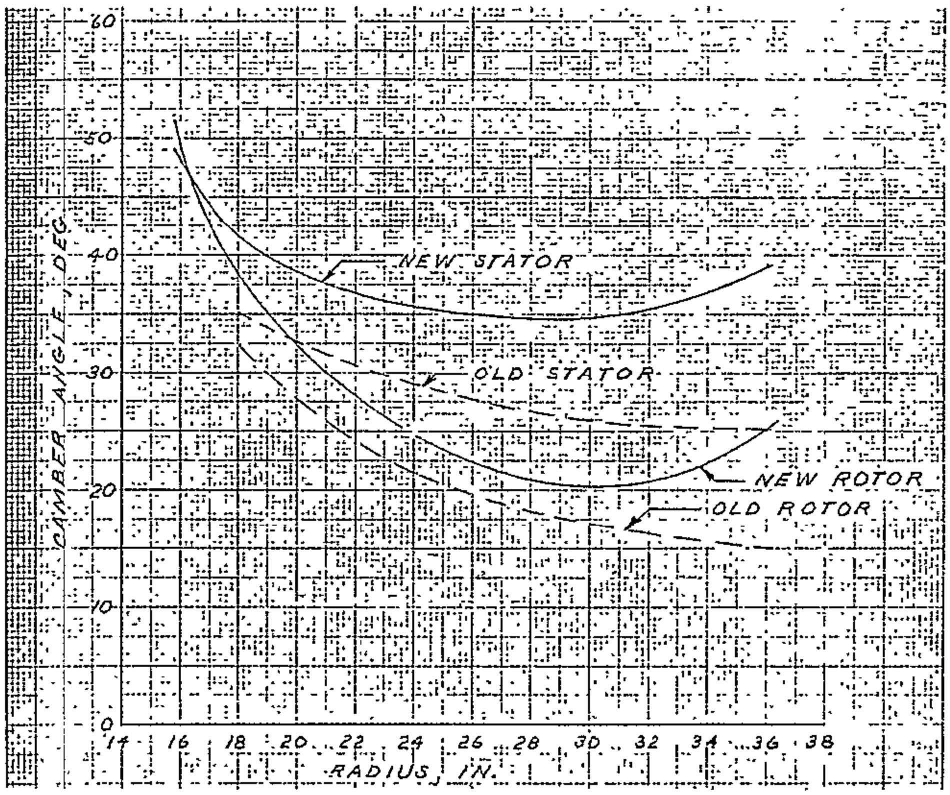

Figure 17. Camber Angle vs. Radius

Blade Stagger

The blade stagger-angle setting (Figure 18) was increased for both rotor and stator. This was largely a consequence of the camber increases shown in Figure 17.

Airfoil Shape Modifications and Blade Stacking Arrangement

The original blade C-4 thickness distribution for the rotor and stator was changed to a modified NACA 65-series thickness distribution on circular arc mean lines, and the individual airfoil sections were stacked on a radial line through their centroids. The rotor blade sections are shown in Figure 19, with the inscribed circle (which is 90% of the blade spacing at the hub) representing the recommended rotor blade trunnion diameter.

The large trunnion size is designed to minimize the clearance that occurs where the root airfoil overhangs the trunnions. Furthermore, since such a clearance at the leading edge tends to form an aerodynamically unfavorable forward-forcing step, it is recommended that the root section be slid aft, as indicated by the dashed line, in order to eliminate any leading edge overhang.

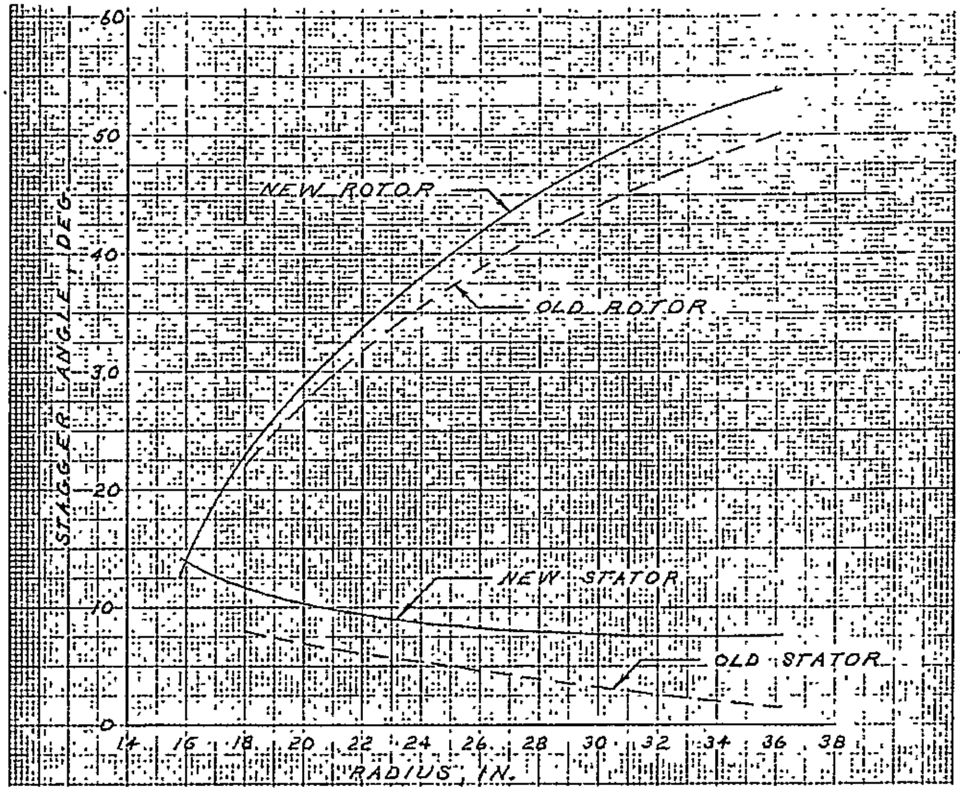

Figure 18. Stagger Angle vs Radius

Hub Modification to Improve End-Wall Boundary Layer

The end-wall boundary layer shape leaving the rotor and entering the stator can be improved by allowing the hub surface between the rotor and stator to rotate. This feature is shown in the view of the fan (Figure 20).

Stator Airfoil Sections

The modified stator airfoil sections are shown in Figure 21. The sections were shaped to discharge the flow to the diffuser without any appreciable swirl.

REDESIGNED FAN PERFORMANCE

The final test results on the redesigned low-speed fan were not forthcoming in time to be incorporated in this report. However, preliminary test results indicate significant performance improvement for the redesigned fan employing 65-series airfoil blade sections over that obtained with the original C-4 airfoil blade section in the low-speed fan design.

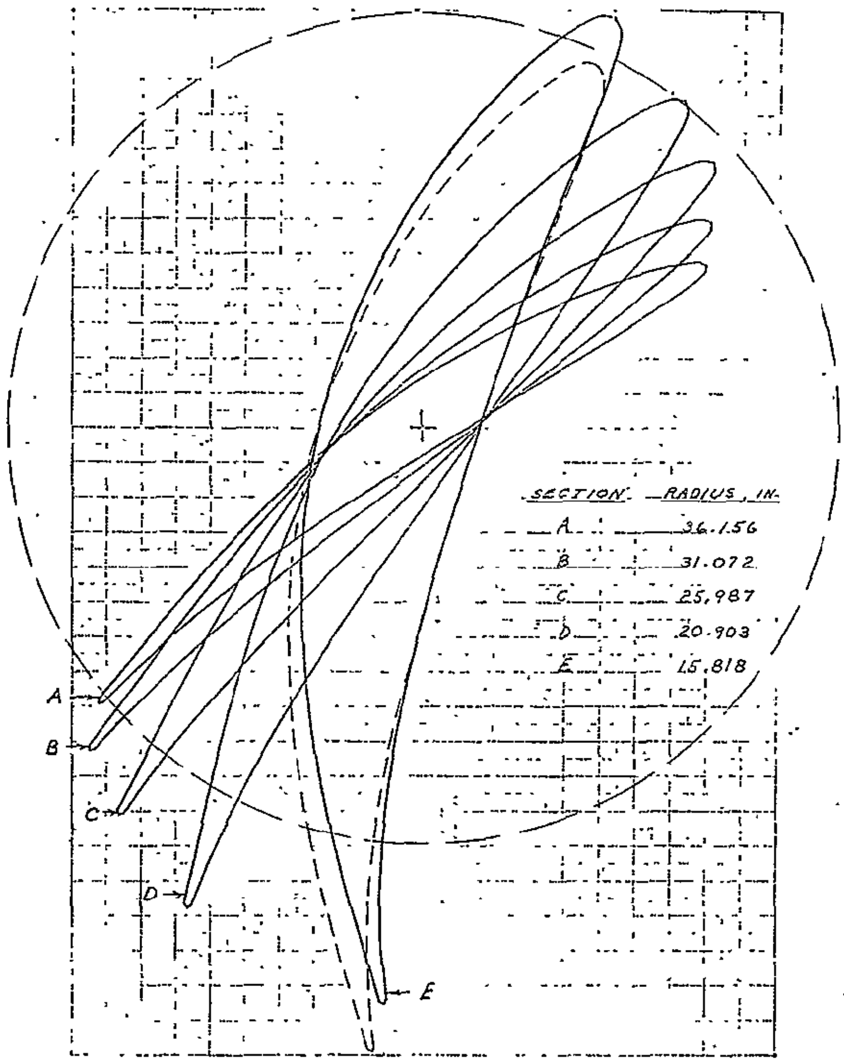

Figure 19. Rotor Blade Sections

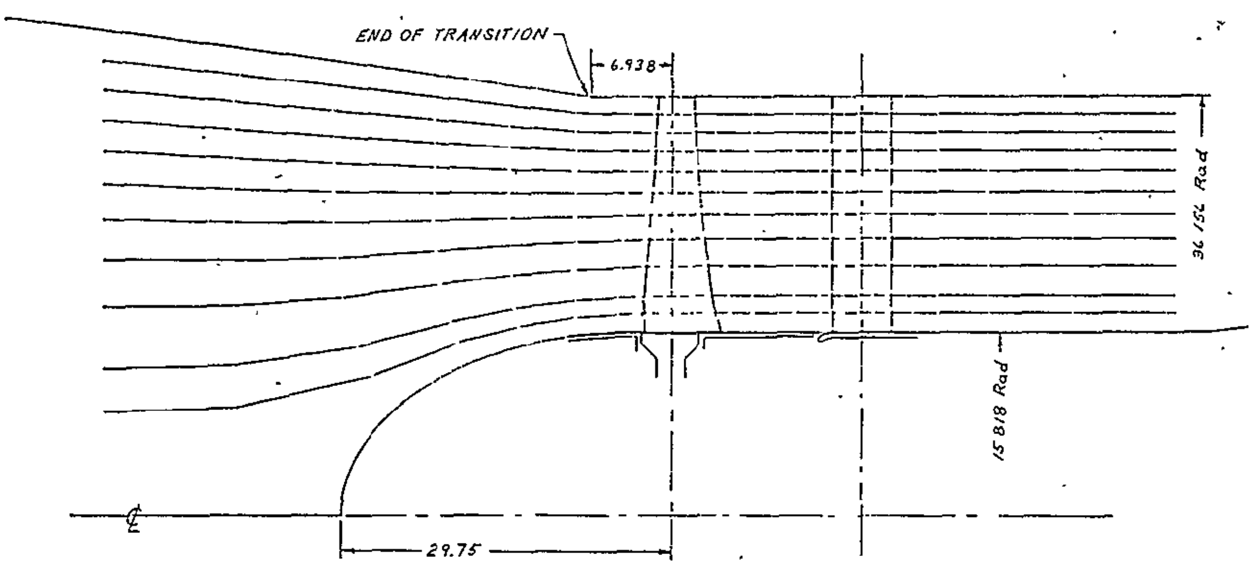

Figure 20. Flow Path

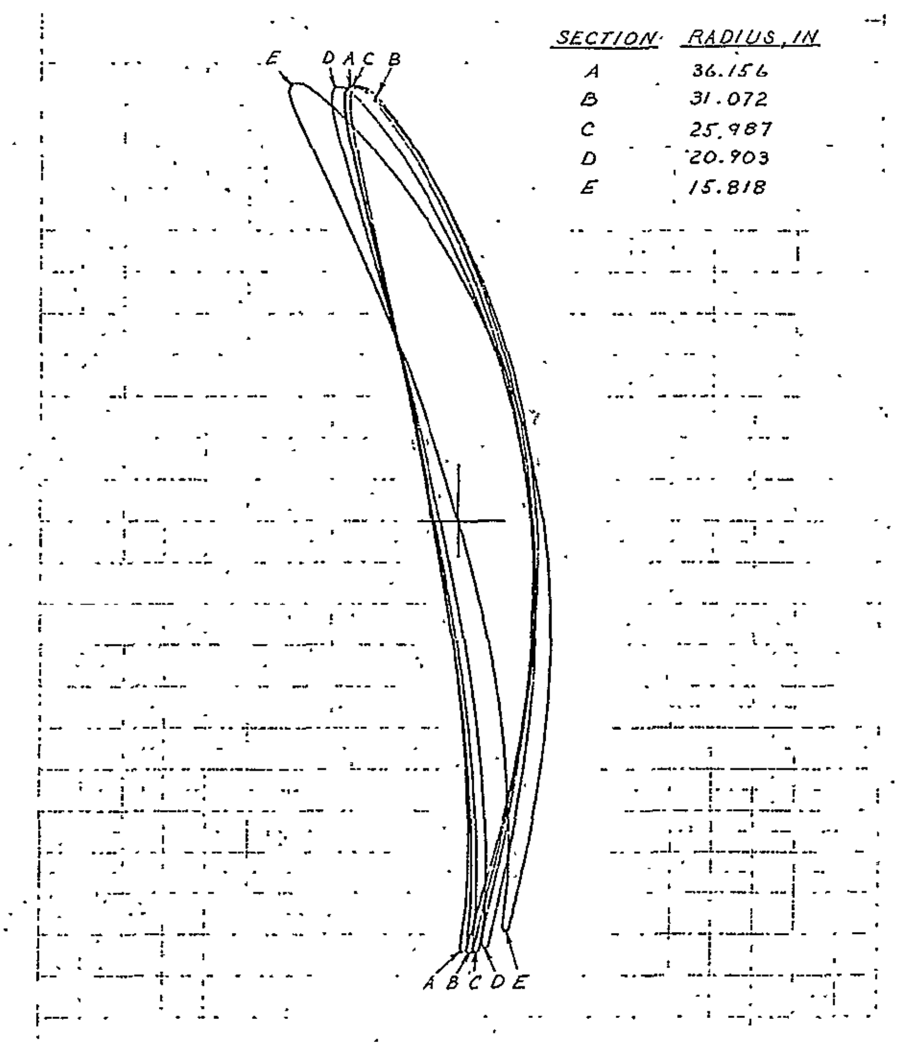

Figure 21. Stator Vane Sections

Section 5

SUMMARY

The comprehensive aero-acoustic investigation program for the NASA-Ames 1/7-scale model fan established the necessary aero-acoustic design guidelines which will enable optimization of the 40 foot full-scale-diameter fans to be incorporated in the repowered section of the 40 x 80 foot wind tunnel. The extensive investigation program established the following fan aero-acoustic characteristics:

1. The low-speed fan design will be quieter than the high-speed fan by 4 to 5 dBA.
2. The high-speed fan with its lighter blade loading was several points more efficient than the low-speed fan. Its indicated efficiency of 86 percent was several points below its objective design efficiency of 90 percent.
3. The original design of the low-speed fan marginally met its design head requirement and was seven percentage points deficient in its efficiency objective. Its poor hub-region operation mandated that a new aerodynamic design be incorporated, if the fan was to meet the performance objectives of the 0.4375 hub/tip ratio design contemplated for the full-scale fans.
4. Initial performance results on the redesigned low-speed fan indicate a significant performance improvement over the original design.
5. Fan inlet distortion tests indicated a considerably greater fan capability in operating with thickened boundary layers over a circumferential sector without stalling.

Section 6

REFERENCES

1. "Large Scale V/STOL Wind Tunnel Power Section Design Study," NASA/Moffett Field Contract NAS2-5890, Marine and Defense Facilities Sales Operation, General Electric Company, November 1970.
2. "Large Scale V/STOL Wind Tunnel Power Section Design Study," NASA/Moffett Field Contract NAS2-5890, Marine and Defense Facilities Sales Operation, General Electric Company, January 7, 1972.
3. "Large Scale V/STOL Wind Tunnel Power Section Design Study," NASA/Moffett Field Contract NAS2-5890 MOD 2, Marine and Defense Facilities Sales Operation, General Electric Company, September 1973.
4. "Feasibility Study of Repowering the 40 x 80 Foot Wind Tunnel and Increasing Its Testing Capacity," John A. Blume and Associates subcontract for NASA-Ames Research Center, Marine and Defense Facilities Sales Operation and Corporate Research and Development, General Electric Company, 1973.
5. "Design of Fans and Model Test Stand for Simulating the Proposed New Fan Power Section of the 40 x 80 NASA/Ames Wind Tunnel," NASA Contract NAS2-7477, Corporate Research and Development, General Electric Company, August 1973.

Appendix A

40 x 80 FOOT MODEL FAN PERFORMANCE INSTRUMENTATION

A. Overall Fan Performance Instrumentation

Stations: 0, $\boxed{1}$, $\boxed{3}$, $\boxed{6}$ and 6A —

$\boxed{}$ Symbols refer to stations described on drawing A T4622-C

Station No.	Type of Instrumentation
0 (Upstream of "STA ZERO")	(1) 5 Thermocouples—Millivolt Readings (2) Barometer—(in. HG) (3) TA—Manometer Fluid Temperature (^{o}F)
$\boxed{1}$	16 - Static Pressure Taps, 4 per Panel (in. H_2O)
$\boxed{3}$	4 - Total Pressure Rakes 6 Total Pressure Tubes per Rake; 24 Total (in. H_2O)
$\boxed{6}$ (4 Circumferential Positions - 90^{o} Apart)	Radial Traverse Probe: (1) Static Pressure (in. H_2O) (2) Total Pressure (in. H_2O) (3) Direction (degrees), Null Balance
6A	3 Fixed Thermocouple Probes for Total Temperature at Strut Entrance

Fan Power Input Measurements:

1. Fan Speed
2. Torque Input, ft-lb

B. Rotor Performance Instrumentation

Stations: 0, $\boxed{1}$, $\boxed{3}$, $\boxed{4}$, $\boxed{5}$ and 6A

Instrumentation for stations 0, $\boxed{1}$, $\boxed{3}$ and 6A same as "Section A"

Instrumentation for stations $\boxed{4}$ and $\boxed{5}$ same as for station $\boxed{6}$ of Section A

C. Diffuser Performance Instrumentation

Stations: 0, $\boxed{1}$, $\boxed{6}$, 6A, and $\boxed{8}$

Instrumentation for stations 0, $\boxed{1}$, $\boxed{6}$ and 6A same as in Section A

PRECEDING PAGE BLANK NOT FILMED

Station No.	Type of Instrumentation
8	16 - Static Pressure Taps, 4 per Panel (in. H_2O)
	4 - Total Pressure Rakes, 6 Total Pressure Tubes per Rake; 24 Total (in. H_2O)

All pressure instrumentation will have to be read to an accuracy of ± 0.01 in. H_2O.

Appendix B

40 x 80 FOOT MODEL FAN OVERALL PERFORMANCE CALCULATION PROCEDURE

PROGRAM STRUCTURE AND INPUT DATA FILE

The program is structured to evaluate the fan adiabatic efficiency, corrected weight flow, and normalized developed head, pressure rise, weight flow, and input horsepower for each specific constant-speed constant-throttle valve flow setting. The program treats each azimuth position of the discharge Radial Traverse Probe as a separate run number. The performance data for the number of azimuth stations employed are normalized and then averaged to arrive at the overall performance data of the fan.

The input data should then be assembled in two arrays. The first array, arbitrarily designated as (I), will correspond to the elements of the Radial Traverse Probe radial positions on centers of equal area at Instrument Station 6 for a particular azimuth location. The second array, arbitrarily designated as (J), will correspond to the azimuth or circumferential positions of the Radial Traverse Probe identified as run numbers.

DATA INPUT FILE

The inputted data for overall performance reduction will be as follows:

(1)	TA(J)	=	Manometer Fluid Temperature, ^{o}F
(2)	BAR(J)	=	Barometric Pressure, "Hg
(3)	TMER(J)	=	Temperature of mercury barometer, ^{o}F
(4)	TO(J)	=	Average of 5 Inlet thermocouples (millivolt readings converted to ^{o}F)
(5)	PSTI(J)	=	Average of 16 static pressure taps at station $\boxed{1}$, "H_2O with respect to ambient
(6)	PTO(J)	=	Average of 24 total pressure tube readings at station $\boxed{3}$, "H_2O with respect to ambient (values should be negative if less than atmospheric pressure)
(7)	PSD(I,J)	=	Static pressure at immersion (I) for azimuth position (J) of Radial Traverse Probe, "H_2O with respect to ambient. Value is negative if pressure is below atmosphere
(8)	PTD(I,J)	=	Total pressure at immersion (I), same as for static pressure in step (7)
(9)	α2Z(I,J)	=	Fluid flow direction with respect to axial direction as measured by Radial Traverse Probe, degrees
(10)	TD(J)	=	Average discharge temperature at station 6A, (millivolt readings converted to ^{o}F)
(11)	N(J)	=	Fan actual speed, rpm
(12)	TORK(J)	=	Fan torque measurement, ft-lb
(13)	NPERC	=	Percent of design speed to which overall performance will be corrected, per unit (100% = 1)
(14)	NDES	=	Fan design speed, rpm

PROGRAM COMPUTATION LOGIC

Two loops will be set up similar to the input data loops, with the (I) loop evaluating the radial pressure data at an azimuth location of the Radial Traverse Probe and the (J) loop evaluating the average conditions of fan efficiency, total head, pressure rise, weight flow, and horsepower associated with all the azimuth measurements of the Radial Traverse Probe, during a particular flow and speed setting.

(005)	AN	=	Inlet Nozzle throat area, ft^2, $S^2 = 6.9^2$
(010)	RD	=	1×10^6 (initially assumed Reynolds number for calculating fan weight flow)
(015)	ETAS	=	0
(020)	HADSUM	=	0
(025)	WSNOR	=	0
(030)	NP	=	Number of azimuth or circumferential positions of Radial Traverse Probe
(035)	NS	=	Number of radial stations of Radial Traverse Probe
(040)	DO 100 J	=	1, NP
(045)	RHOW	=	Manometer fluid density, lb/ft^3 expressed as a function of TA(J) (RHOW = 62.38 lb/ft^3 at 58^oF)
(050)	KPS	=	Pressure conversion factor ("H_2O to psi) RHOW/1728 = (045)/1728
(055)	KMER	=	Barometer multiplication factor to convert "Hg to psi, function of TMER(J) = (3→ Data)
(060)	PATM(J)	=	Absolute pressure in psia, KMER x BAR(J) = (055) x (2→ Data)
(065)	TOA(J)	=	Absolute inlet air temperature, ^oR
(070)	RHO	=	Inlet density, lb/ft^3, $\frac{PATM(J)}{TOA(J)} \times 2.7 = \frac{(060)}{(065)} \times 2.7$
(075)	DPN	=	Inlet Nozzle differential pressure, psi, PSTI(J) x KPS = (5→ Data) x (050)
(080)	MU	=	Dynamic Viscosity, lb/sec-ft $[1.109 + 1.673 \times 10^{-3}\ TO(J)] \times 10^{-5} =$ $1.109 + 1.673 \times 10^{-3}\ (4 \rightarrow Data) \quad \times 10^{-5}$
(085)	CN	=	Nozzle flow coefficient, CN = f(RD) (Equation for CN to be developed from 1 ft^2. Inlet Bellmouth Flow Tests at GE)
(090)	WN(J)	=	Fan weight flow, lb/sec, CN x AN x $12 \times \sqrt{DPN \times RHO \times 2g} = 96.26 \times (085) \times (005) \times [(075) \times (070)]^{1/2}$
(095)	RDN	=	$\frac{WN(J)}{(SxMU)}$ = (090)/(6.9 x (080))
(100)	If [ABS(RDN - RD) · GT · 500) Gϕ Tϕ (110)		
(105)	Gϕ Tϕ (115)		
(110)	RD	=	RDN, Return to (085)
(115)	PTOA(J)	=	Absolute inlet total pressure, psia, (PATM(J) + PTO(J) x KPS) = [(060) + (6→ Data) x (050)]

Evaluation of Radial Weighted Flow Discharge Total Pressure as Measured by Radial Traverse Probe at Station [6].

(120)	WSUM(J)	=	0
(125)	PTDSUM	=	0
(130)	PTDWSUM	=	0
(135)	DO 200, I	=	1, NS
(140)	PSDA(I,J)	=	Absolute discharge static pressure, psia, (PATM(J) + PSD(I,J) x KPS) = [(060) + (7→ Data) x (050)]
(145)	PTDA(I,J)	=	Absolute total pressure, psia, (PATM(J) + PTD(I,J) x KPS) = [(060) + (8→ Data) x (050)]
(150)	TDR(J)	=	Discharge temperature, ^oR, [TD(J) + 460] = (10→ Data) + 460
(155)	VAB(I,J)	=	Absolute velocity, ft/sec, (2g R (TDR) $\left[\frac{PTDA(I,J)}{PSDA(I,J)}\right] - 1$) = 58.56 $\left[(150) \times \frac{(145)}{(140)} - 1)\right]^{1/2}$
(160)	α2Z(I,J)	=	Fluid flow direction with respect to axial direction, degrees
(165)	VZ(I,J)	=	Axial component of absolute velocity, ft/sec, [VAB(I,J) x cosα 2Z(I_2,J)] = (155) x cos (160)
(170)	AZI	=	Stream tube area, ft^2, $\frac{\pi}{4} \left(\frac{DT^2 - DH^2}{NS}\right)$ = $0.785\left(\frac{6^2 - 3^2}{NS}\right) = \frac{21.206}{(035)}$
(175)	RHOD(I,J)	=	Approximate stream discharge density, lb/ft^3, $\left[2.7 \times \frac{PSDA(I,J)}{TDR(J)}\right] = 2.7 \frac{(140)}{(150)}$
(180	W(I,J)	=	Stream tube weight flow, lb/sec, RHOD(I,J) x VZ)I,J) x AZI = (175) x (165) x (170)
(185)	WSUM(J)	=	WSUM(J) + W(I,J) = (120) + (180)
(190)	PTDW(I,J)	=	Weighted total pressure term in stream tube, (psia) (lb/sec), PTDA(I,J) x W(I,J) = (145) x (180)
(195)	PTDWSUM	=	PTDWSUM + PTDW(I,J) = (130) + (190)
(200)	PTDSUM	=	PTDSUM + PTDA(I,J) - (125) $\pm$ (145)
(205)	200 continue		
(210)	If (ABS (1 $\frac{WSUM(J)}{Wn(J)}$	.GT.	.15) Gϕ Tϕ (222)
(215)	PTDJ(J)	=	PTDWSUM/WSUM(J) = (195)/(185)
(220)	GO TO(230)		
(222)	Print Message: Weighted Method Not Used		
(225)	PTDJ(J)	=	PTDSUM/NS = (200)/(035)
(230)	DEL	=	Ratio of inlet total pressure to standard pressure of 14.694 lb/in^2, [PTOA(J)/14.694] = (115)/14.694

(235) THETA = Ratio of inlet total temperature to standard temperature of 518.6°R [TOA(J)/518.6] = (065)/518.6

(240) SQTHET = $(\text{THETA})^{1/2} = (235)^{1/2}$

(245) NCOR(J) Corrected speed, rpm, $N(J)/\sqrt{\theta}$ = (11→ Data/(240)

(250) KN = Speed and temperature correction factor (Fan design speed) x NPERC/NCOR(J) = (14→ Data) x (13→ Data)/(245)

(255) WCOR(J) = Corrected Flow, lb/sec, [WN(J) x SQTHET/DEL] = (090) x (240)/(230)

(260) WNOR(J) = Normalized weight flow, lb/sec, WN(J) x KN/DEI = (090) x (240)/(230)

(265) WSNOR = Weight flow summation, lb/sec, WSNOR + WNOR(J) = (025) + (260)

(270) PR(J) = Pressure ratio at azimuth position of Radial Traverse Probe, [PTD(J)/PTOA(J)] = (215)/(115) or (225)/(115)

(275) HISEN = Isentropic developed head, ft, $[PR(J)^{.286} - 1]$ x TOA(J) x 186.6 = $[(270)^{.286} - 1]$ x (065) x 186.6)

(280) HISNOR(J) = Normalized developed head, ft, $[\text{HISEN} \times \text{KN}^2]$ = $(275) \times (250)^2$

(285) HADSUM = Head summation, ft, [HADSUM + HISNOR(J)] = (020) + (280)

(290) HPINP(J) = Shaft power input, HP, [TORK(J) x 2π N(J)/33,000] = (12→ Data) (11→ Data) x 1.904×10^{-4}

(295) ETA(J) = Fan efficiency, $\frac{\text{WN(J)} \times \text{HISEN}}{\text{HPINP(J)} \times 550}$ = (090) x (275)/[(290) x 550]

(300) ETAS = Efficiency summation, [ETAS = ETA(J)] = (015) + (295)

(305) 100 continue

(310) ETAV = Average fan adiabatic efficiency for all azimuth position of Traverse Probe,

$$\left(\frac{\text{ETAS}}{\text{NP}}\right) = (300)/(300)$$

(315) HADAV = Average fan developed adiabatic head, ft, for all azimuth position of Traverse Probe, (HADSUM/NP) = (285)/(030)

(320) WNORAV = Average normalized weight flow, lb/sec, for all azimuth positions of Traverse Probe, (WSNOR/NP) = (265)/(030)

(325) DPFAN = Average fan developed pressure, lb/ft^2,

$$= 2116 \left[\frac{\text{HADAV}}{(186.6) \times 518.6} + 1\right]^{3.5} - 1$$

$$= \left[(315) \times 1.03337 \times 10^{-5} + 1^{\ 3.5} - 1\right]$$

(330) HPAV = Average fan shaft power, hp, HADAV x WNORAV/ [ETAV x 550] = (315) x (320)/ [(310) x 550]

DESIRED COMPUTER PRINT-OUTS

1. All Input Data Except TA(J) and TMER(J)

2. The following list of calculated results

PATM(J)	WN(J)	HISNOR(J)	WSUM(J)
TOA(J)	WCOR(J)	HPIND(J)	
PTOA(J)	WNOR(J)	ETA(J)	
TDR(J)	PR(J)		
PTDJ(J)			
ETAV,	HADAV,	WNORAV	
	DPFAN	HPAV	

Appendix C

FAN ACOUSTIC DATA REDUCTION PROGRAM

```
NASAFAN      10/29/74

10 FILES CØNTRØL;ATTENS;FANDATA;MIKEAREA;PAGE;FANCALC
20 DIM X(1,36),A(1,36),R(1,36),F(1,36),C(4,36),M(4,36),K(1,36),V(1,36)
30 DIM P(36,36),Z(10),L(36,37),W(36,36),T(1,37),O(1,37),S(1,36),U(1,36)
40 SCRATCH #6
50 MARGIN #6,175
60 MAT READ #0,F,R,S,U
70 A0 = 100
80 C0 = -10.5
90 S0 = .15
100 Y0 = SGN(LØG(S0))*INT(ABS(3/LØG(2)*LØG(S0))+.5)
110 W0 = 6/S0↑2
120 N = 36
130 MAT READ #1,X(1,N)
140 MAT READ #2,A(1,N)
150 READ #3,T$
160 MAT READ #4,M
170 MAT READ #4,K
180 READ #5,P$
190 READ #0,A$,B$,C$,D$,E$,F$,G$,H$,I$,J$
200 READ #3,Q
210 IF Q > 0 THEN 1860
220 Q = -Q
230 J2 = INT(Q)
240 J1 = 100*(Q-J2)
250 J1 = INT(J1-.5)
260 J2 = INT(J2-.5)
270 FØR J = J1 TØ J2
280 READ #3,C(1,J)
290 NEXT J
300 Z(1) = C(1,11)
310 FØR K = 2 TØ 4
320 READ #3,Q0
330 IF Q0 <> -Q THEN 1860
340 FØR J = J1 TØ J2
350 READ #3,C(K,J)
360 NEXT J
370 Z(K) = C(K,11)
380 NEXT K
390 FØR K = 1 TØ N
400 READ #3,Q0
410 IF Q0 <> -Q THEN 1860
420 FØR J = J1 TØ J2
430 READ #3,P(K,J)
440 M0 = K-4*INT((K-1)/4)
450 L(X(1,K),J) = P(K,J)-M(M0,J)+124-Z(M0)+A(1,K)-A0
460 W(X(1,K),J) = L(X(1,K),J)+K(1,X(1,K))+C0
470 V(1,J) = L(X(1,K),J)
480 NEXT J
490 GØSUB 1660
500 L(X(1,K),37) = A9
```

PRECEDING PAGE BLANK NOT FILMED

NASAFAN 10/29/74

```
510 NEXT K
520 FØR J = J1 TØ J2
530 W = 0
540 FØR K = 1 TØ N
550 W = W+10↑(W(K,J)/10)
560 NEXT K
570 T(1,J) = 10/LØG(10)*LØG(W)
580 NEXT J
590 FØR J = J1 TØ J2
600 IF J > J2+Y0 THEN 630
610 Q(1,J) = T(1,J-Y0)+10/LØG(10)*LØG(W0)
620 NEXT J
630 FØR J = J1 TØ J2
640 V(1,J) = T(1,J)
650 NEXT J
660 GØSUB 1660
670 T(1,37) = A9
680 FØR J = J1 TØ J2
690 V(1,J) = Q(1,J)
700 NEXT J
710 GØSUB 1660
720 Q(1,37) = A9
730 FØR J = 1 TØ 10
740 PRINT #6
750 NEXT J
760 PRINT #6,USING780,T$
770 PRINT #6
780:'CCCCCCCCCCCCCCCCCCCCCCCCCCCCCCCCCCCCCCCCCCCCCCCCCCCCCCCCCCCCCCCCCCCCCC
790 PRINT #6
800 PRINT #6
810 PRINT #6,A$;TAB(21);B$
820 PRINT #6
830 PRINT #6,TAB(2);C$;TAB(20);D$;TAB(30);F$
840 PRINT #6,TAB(30);F$
850 PRINT #6
860 FØR J = J1 TØ J2
870 PRINT #6,USING 1530,F(1,J);
880 GØTØ 910
890 PRINT #6
900 PRINT #6,"   ";J$;" ";
910 PRINT #6,"          ";
920 PRINT #6,USING 930,T(1,J);
930: ###.##
940 PRINT #6,"      ";
950 IF J = 37 THEN 970
960 IF J > J2+Y0 THEN 980
970 PRINT #6,USING 930,Q(1,J);
980 PRINT #6
990 IF J = 37 THEN 1030
1000 NEXT J
```

NASAFAN 10/29/74

```
1010 J = 37
1020 GØTØ 890
1030 PRINT #6,P$
1040 FØR J = 1 TØ 10
1050 PRINT #6
1060 NEXT J
1070 PRINT #6,USING 1080,G$
1080:'CCCCCCCCCCCCCCCCCCCCCCCCCCCCCCCCCCCCCCCCCCCCCCCCCCCCCCCCCCCCCCCCCCCCCC
1090 PRINT #6
1100 PRINT #6
1110 A = 1
1120 B = 4
1130 GØSUB 1330
1140 FØR J = 1 TØ 10
1150 PRINT #6
1160 NEXT J
1170 PRINT #6,USING 1080,H$
1180 PRINT #6
1190 PRINT #6
1200 A = 5
1210 B = 16
1220 GØSUB 1330
1230 FØR J = 1 TØ 10
1240 PRINT #6
1250 NEXT J
1260 PRINT #6,USING 1080,I$
1270 PRINT #6
1280 PRINT #6
1290 A = 17
1300 B = 36
1310 GØSUB 1330
1320 STØP
1330 PRINT #6,A$;" ";
1340 FØR I = A TØ B
1350 PRINT #6,USING 1360,S(1,I);
1360:     ##
1370 NEXT I
1380 PRINT #6
1390 PRINT #6,TAB(2);C$;"      ";
1400 FØR I = A TØ B
1410 IF U(1,I) <> 1 THEN 1440
1420 PRINT #6,"  **  ";
1430 GØTØ 1450
1440 PRINT #6,"      ";
1450 NEXT I
1460 PRINT #6
1470 PRINT #6
1480 FØR J = J1 TØ J2
1490 PRINT #6,USING 1530,F(1,J);
1500 GØTØ 1530
```

NASAFAN 10/27/74

```
1510 PRINT #6
1520 PRINT #6,"    ";J$;" ";
1530:   #####
1540 PRINT #6,"      ";
1550 FØR I = A TØ B
1560 PRINT #6,USING 1570,L(S(1,I),J);
1570: ###.#
1580 NEXT I
1590 PRINT #6
1600 IF J = 37 THEN 1640
1610 NEXT J
1620 J = 37
1630 GØTØ 1510
1640 PRINT #6,P$
1650 RETURN
1660 A9 = 0
1670 FØR J = 1 TØ 31
1680 A9 = A9+10↑((V(1,J)-R(1,J))/10)
1690 NEXT J
1700 A9 = 10/LØG(10)*LØG(A9)
1710 RETURN
1720 DATA 25,31,40,50,63,80,100,125,160,200,250,315,400,500,630,800
1730 DATA 1000,1250,1600,2000,2500,3150,4000,5000,6300,8000,10000
1740 DATA 12500,16000,20000,25000,31500,40000,50000,63000,80000
1750 DATA 44.7,39.4,34.6,30.2,26.2,22.5,19.1,16.1,13.4,10.9,8.6
1760 DATA 6.6,4.8,3.2,1.9,.8,0,-.6,-1,-1.2,-1.3,-1.2,-1,-.5,.1
1770 DATA 1.1,2.5,4.3,6.6,9.3,0,0,0,0,0,0
1780 DATA 15,16,22,21,8,9,10,11,17,23,29,28,27,26,20,14,1,2,3,4,5,6
1790 DATA 12,18,24,30,36,35,34,33,32,31,25,19,13,7
1800 DATA 1,1,1,1,1,0,0,1,0,0,1,0,0,1,0,0,1,0,0,0,0,1,0,0,0,0,1
1810 DATA 0,0,0,0,1,0,0,0,0
1820 DATA FREJUENCY,LW RE 1E-12 WATTS,HERTZ,MØDFL,PRØTØTYPF
1830 DATA (SIX FANS)
1840 DATA SPL ØF CENTER CELLS,SPL ØF INTERMFDIATF CFLLS
1850 DATA SPL ØF ØUTER CFLLS,DBA
1860 PRINT "CHFCKDATA"
1870 END
```

```
CØNTRØL      10/29/74

100 1,4,7,10,2,5,8,11,3,6,9,12
110 13,16,19,22,14,17,20,23,15,18,21,24
120 25,28,31,34,26,29,32,35,27,30,33,36


ATTENS       10/29/74

100 90,90,90,90,90,90
110 90,90,90,90,90,90
120 90,90,90,90,90,90
130 90,90,90,90,90,90
140 90,90,90,90,90,90
150 90,90,90,90,90,90
```

FANDATA 10/29/74

```
50 PRØGRAM CALCULATIØN CHECKS
100     -30.02,070.00,070.00,070.00,070.50,086.25,070.00,070.00,
110     077.00,086.00,104.00,123.50,105.00,086.75,089.00,073.75,
120     070.00,075.00,070.00,070.00,070.00,070.00,070.00,070.00,
130     070.00,070.00,070.00,070.00,070.00,070.00,
140     -30.02,070.00,070.00,070.00,070.50,086.25,070.00,070.00,
150     077.00,086.00,104.00,123.50,105.00,086.75,089.00,073.75,
160     070.00,075.00,070.00,070.00,070.00,070.00,070.00,070.00,
170     070.00,070.00,070.00,070.00,070.00,070.00,
180     -30.02,070.00,070.00,070.00,070.50,086.25,070.00,070.00,
190     077.00,086.00,104.00,123.50,105.00,086.75,089.00,073.75,
200     070.00,075.00,070.00,070.00,070.00,070.00,070.00,070.00,
210     070.00,070.00,070.00,070.00,070.00,070.00,
220     -30.02,070.00,070.00,070.00,070.50,086.25,070.00,070.00,
230     077.00,086.00,104.00,123.50,105.00,086.75,089.00,073.75,
240     070.00,075.00,070.00,070.00,070.00,070.00,070.00,070.00,
250     070.00,070.00,070.00,070.00,070.00,070.00,
260     -30.02,078.25,078.00,073.25,073.25,072.00,070.00,070.00,
270     075.25,080.75,075.00,080.00,088.00,094.00,095.50,092.75,
280     096.75,105.75,095.00,095.75,098.75,096.00,095.00,094.50,
290     094.00,092.00,092.00,090.50,088.50,090.75,
300     -30.02,090.25,086.25,081.50,078.25,074.50,073.25,072.75,
310     078.00,084.50,080.50,084.25,088.50,092.50,094.00,091.50,
320     099.00,111.00,096.50,100.00,098.75,097.25,099.00,096.25,
330     096.75,095.50,093.00,090.50,089.75,086.50,
340     -30.02,078.25,078.00,073.75,073.00,072.75,071.75,070.00,
350     071.50,081.25,075.50,079.50,086.75,091.25,093.00,089.50,
360     093.25,105.50,091.25,095.00,095.25,093.50,095.00,090.50,
370     088.25,086.25,084.75,083.00,086.50,085.75,
380     -30.02,078.75,078.00,072.50,074.00,073.25,071.50,070.00,
390     073.50,085.75,074.50,079.00,086.50,090.00,091.50,090.75,
400     095.00,107.25,091.75,095.00,097.25,092.50,094.75,089.75,
410     086.75,085.25,083.25,081.75,082.00,081.25,
420     -30.02,079.50,076.50,073.25,071.75,071.00,070.75,070.00,
430     073.25,087.00,074.25,079.25,087.50,092.00,094.25,091.25,
440     095.75,108.25,093.75,094.50,098.50,095.25,095.50,090.00,
450     088.75,087.00,085.25,082.75,082.00,083.50,
460     -30.02,080.00,079.00,073.25,073.75,072.75,070.00,070.00,
470     074.50,075.00,081.00,081.75,089.50,095.75,096.75,096.25,
480     096.75,107.00,103.00,099.50,100.50,100.25,099.50,097.00,
490     098.00,096.75,096.25,095.50,092.50,094.00,
500     -30.02,099.25,094.75,091.00,087.25,085.50,083.50,078.50,
510     081.50,081.25,090.00,086.75,090.75,094.50,095.25,094.50,
520     099.00,109.25,108.75,104.00,102.25,102.25,103.50,100.75,
530     100.75,099.50,098.00,095.50,094.00,090.50,
540     -30.02,077.50,078.50,073.00,073.25,072.50,071.00,070.00,
550     072.25,076.00,085.75,081.75,087.75,094.25,094.50,093.25,
560     093.50,104.00,104.00,099.25,099.00,098.00,096.75,093.75,
570     092.75,090.75,089.50,087.75,088.50,087.00,
580     -30.02,079.25,077.25,073.75,073.25,072.50,071.25,070.25,
```

ORIGINAL PAGE IS OF POOR QUALITY

FANDATA 10/29/74

```
590     075.25,078.50,088.00,080.50,085.50,093.25,092.50,094.00,
600     096.75,104.00,102.50,098.50,100.25,097.00,098.75,093.00,
610     091.50,090.00,088.25,086.50,035.75,084.75,
620     -30.02,079.00,077.50,074.25,071.50,070.75,071.75,070.00,
630     071.50,075.75,085.50,080.00,087.75,095.00,095.50,095.00,
640     096.25,104.50,103.75,098.00,100.00,099.50,097.25,093.75,
650     093.00,091.00,089.75,087.50,086.00,086.75,
660     -30.02,078.50,079.50,073.00,072.25,072.50,071.00,073.75,
670     079.00,086.75,091.00,095.75,098.75,097.00,097.00,101.50,
680     097.50,095.00,095.50,098.00,101.75,095.25,094.25,094.00,
690     095.75,093.50,094.50,093.50,091.75,093.75,
700     -30.02,079.75,076.75,074.00,072.75,071.00,072.50,074.75,
710     077.50,084.50,091.75,093.00,095.75,094.50,094.25,098.25,
720     096.50,093.25,093.25,095.75,097.25,090.00,091.50,087.75,
730     086.75,086.00,085.50,086.00,087.50,083.25,
740     -30.02,080.50,077.50,074.00,072.75,073.75,071.75,073.50,
750     076.50,080.00,085.75,092.75,096.25,093.50,094.75,095.00,
760     093.25,091.25,088.50,093.75,098.00,091.25,089.25,089.25,
770     087.00,085.00,086.00,084.25,087.25,086.75,
780     -30.02,082.00,078.50,073.50,073.50,073.00,071.50,073.50,
790     077.25,082.25,088.50,094.00,095.50,093.75,094.25,097.00,
800     094.50,091.75,092.75,095.25,098.75,091.75,095.75,091.25,
810     088.75,088.00,085.75,085.50,085.50,094.50,
820     -30.02,081.75,077.75,072.75,075.50,073.00,072.50,074.75,
830     078.00,084.50,089.25,093.25,096.00,095.25,093.25,098.50,
840     097.25,094.50,092.50,095.00,099.50,092.00,091.00,090.75,
850     088.75,088.00,086.75,084.25,083.75,084.75,
860     -30.02,079.50,079.50,073.75,074.00,074.75,075.25,078.00,
870     081.25,086.50,092.50,092.50,090.50,089.25,090.25,090.25,
880     094.25,108.50,103.00,096.00,094.75,094.00,093.50,089.75,
890     088.50,085.75,082.50,080.25,076.75,075.00,
900     -30.02,079.00,078.75,074.25,074.50,075.50,078.50,082.50,
910     085.25,089.00,094.50,095.75,094.75,092.50,092.00,093.75,
920     097.00,109.00,108.50,102.25,098.50,100.25,100.25,098.00,
930     098.75,097.75,095.50,093.25,091.75,088.50,
940     -30.02,079.25,078.75,073.75,073.50,074.50,075.25,079.50,
950     082.00,085.75,092.75,092.25,091.75,088.25,089.25,090.25,
960     095.25,106.50,103.50,096.75,096.00,096.25,098.00,090.75,
970     089.25,087.00,085.00,082.25,080.00,076.50,
980     -30.02,080.50,077.75,074.00,074.25,074.00,073.75,075.50,
990     077.25,082.75,091.75,090.00,087.50,084.00,088.00,090.75,
1000    093.75,103.00,101.00,093.75,090.75,089.50,090.00,086.75,
1010    084.75,082.25,080.00,079.00,077.50,075.50,
1020    -30.02,080.25,076.75,074.00,074.00,072.50,074.25,078.25,
1030    081.00,084.00,089.25,091.00,089.25,089.25,090.75,091.25,
1040    097.50,107.50,106.75,097.25,092.50,095.00,094.00,087.00,
1050    087.50,086.50,083.75,081.50,079.75,080.50,
1060    -30.02,080.00,079.50,073.75,073.00,070.75,071.75,072.00,
1070    075.00,074.50,076.25,076.25,077.00,078.00,084.50,088.00,
1080    087.75,090.00,088.00,087.75,083.50,077.25,079.25,079.50,
```

FANDATA 10/29/74

```
1090    077.50,075.50,074.75,072.50,072.50,071.75,
1100    -30.02,079.75,079.50,074.50,075.25,071.75,071.50,073.50,
1110    075.50,075.75,080.50,077.50,076.75,078.75,084.75,091.25,
1120    087.00,089.50,090.50,089.50,083.75,078.50,078.50,078.25,
1130    078.00,075.75,077.00,077.50,073.00,072.75,
1140    -30.02,079.75,078.25,072.75,073.25,073.25,071.00,071.00,
1150    073.00,080.00,090.50,076.50,077.75,080.25,081.25,084.75,
1160    085.50,086.50,087.50,086.75,085.75,082.25,086.00,080.75,
1170    081.25,081.00,079.25,077.00,077.25,074.50,
1180    -30.02,079.50,078.75,074.00,073.75,071.75,072.75,073.25,
1190    076.00,081.00,091.00,079.25,079.00,079.50,086.50,091.75,
1200    087.50,090.50,090.75,089.25,083.25,082.25,084.75,085.75,
1210    082.25,081.00,080.00,079.75,077.75,077.50,
1220    -30.02,081.50,077.25,073.50,073.00,071.75,072.75,074.50,
1230    077.00,077.00,082.50,079.50,080.00,083.75,086.75,088.50,
1240    088.25,090.00,088.75,091.50,086.00,082.00,087.25,081.75,
1250    081.25,079.75,078.00,078.25,078.00,080.25,
1260    -30.02,081.50,078.75,073.50,074.25,073.75,073.75,077.25,
1270    080.25,086.00,097.00,099.25,102.00,100.75,100.25,109.25,
1280    102.00,097.50,097.50,102.00,106.25,100.75,099.25,099.25,
1290    100.00,097.25,097.00,097.25,095.00,095.75,
1300    -30.02,081.50,078.50,074.50,073.50,071.25,072.50,077.50,
1310    079.75,085.00,096.25,095.75,098.50,096.75,096.50,105.50,
1320    099.25,096.00,098.00,099.25,101.50,096.25,094.75,088.50,
1330    086.50,087.75,090.00,089.75,087.75,085.50,
1340    -30.02,078.50,079.00,073.00,073.75,074.25,073.00,076.25,
1350    079.00,084.00,089.00,095.00,098.75,095.75,094.25,104.00,
1360    096.00,095.50,095.00,099.00,103.00,099.75,094.00,094.00,
1370    090.75,089.75,090.50,089.00,090.75,089.00,
1380    -30.02,080.75,076.50,072.75,073.75,072.00,073.50,077.75,
1390    080.00,085.00,093.25,096.50,098.50,095.75,094.00,102.25,
1400    097.25,095.00,096.25,101.25,102.25,099.00,097.25,092.00,
1410    092.00,093.25,091.75,090.50,088.25,086.00,
1420    -30.02,081.75,079.00,073.25,072.75,074.75,074.50,077.50,
1430    079.75,086.00,096.75,098.00,099.00,096.00,095.50,104.75,
1440    101.75,097.50,097.75,100.25,103.00,101.00,096.75,095.75,
1450    094.25,092.75,091.50,090.50,089.50,089.50,
1460    -30.02,080.00,080.75,074.00,075.00,075.75,077.00,080.75,
1470    085.00,089.50,095.50,095.75,094.25,092.00,091.25,096.25,
1480    097.50,104.75,104.50,101.25,097.00,096.50,096.25,093.25,
1490    092.75,089.75,087.25,084.75,081.00,079.00,
1500    -30.02,078.25,077.00,074.75,075.50,077.50,081.75,086.75,
1510    089.50,093.75,096.75,093.00,097.25,095.25,093.75,098.00,
1520    099.75,109.00,110.00,106.00,100.50,103.50,104.50,102.50,
1530    103.00,102.25,100.50,098.25,096.25,093.50,
1540    -30.02,079.75,079.00,074.25,074.25,075.75,078.25,084.75,
1550    086.50,090.25,095.75,096.25,095.25,091.25,091.25,095.75,
1560    098.50,107.50,104.25,101.00,098.00,098.50,096.50,094.75,
1570    093.25,090.75,089.00,086.25,083.50,080.50,
1580    -30.02,080.75,075.50,074.00,073.50,072.25,075.00,078.75,
```

```
FANDATA      10/29/74

1590     080.50,085.25,096.00,094.75,091.50,088.25,087.25,094.25,
1600     098.00,104.50,104.00,100.00,094.50,093.75,094.00,091.25,
1610     088.50,086.50,083.25,083.50,080.50,079.50,
1620     -30.02,081.25,077.25,073.75,072.25,073.25,077.00,082.25,
1630     083.50,087.75,093.00,093.00,091.00,092.25,091.50,095.25,
1640     099.75,107.50,107.00,101.25,094.00,098.75,098.25,090.75,
1650     090.25,089.75,088.00,085.00,082.00,078.75,
1660     -30.02,080.50,077.50,072.00,073.75,072.00,072.00,074.25,
1670     075.75,076.25,083.25,079.75,079.00,080.75,084.75,091.75,
1680     090.75,093.25,093.00,090.50,086.00,084.00,081.75,081.00,
1690     080.00,077.75,076.25,076.00,076.00,075.25,
```

```
MIKEAREA     10/29/74

100 0,0,0,0,0,0,0,0,0,0,0,0,0,0,0,0,0,0,0,0,0,0,0,0,0,0,0,0,0,0,0,0,0,0,0,0
110 0,0,0,0,0,0,0,0,0,0,0,0,0,0,0,0,0,0,0,0,0,0,0,0,0,0,0,0,0,0,0,0,0,0,0,0
120 0,0,0,0,0,0,0,0,0,0,0,0,0,0,0,0,0,0,0,0,0,0,0,0,0,0,0,0,0,0,0,0,0,0,0,0
130 0,0,0,0,0,0,0,0,0,0,0,0,0,0,0,0,0,0,0,0,0,0,0,0,0,0,0,0,0,0,0,0,0,0,0,0
200 10,10,10,10,10,10
210 10,10,10,10,10,10
220 10,10,10,10,10,10
230 10,10,10,10,10,10
240 10,10,10,10,10,10
250 10,10,10,10,10,10
```

****

R.J.WELLS1 FANCALC 10/29/74 12:22

****

PROGRAM CALCULATION CHECKS

FREQUENCY HERTZ	LW RE 1E-12 WATTS MODEL	PROTOTYPE (SIX FANS)
25	91.11	115.19
31	87.55	121.59
40	83.40	122.66
50	81.43	124.10
63	80.49	123.31
80	80.67	123.39
100	83.54	128.77
125	86.20	126.69
160	90.93	134.64
200	97.33	132.18
250	98.40	128.75
315	99.84	128.88
400	99.05	126.94
500	99.13	126.55
630	104.51	123.94
800	102.44	123.85
1000	110.38	122.51
1250	107.92	121.25
1600	104.49	119.72
2000	104.62	118.20
2500	102.68	117.46
3150	102.29	
4000	99.68	
5000	99.59	
6300	98.25	
8000	96.99	
10000	95.46	
12500	93.94	
16000	93.20	
DBA	115.80	132.82

SPL OF INTERMEDIATE CELLS

FREQUENCY HERTZ	8 **	9	10	11 **	17	23	29 **	28	27	26 **	20	14
25	89.7	69.0	69.2	68.0	69.7	70.7	72.2	72.0	70.2	71.2	71.0	69.5
31	85.2	70.0	68.5	69.0	69.2	67.2	69.5	69.2	69.5	67.0	68.2	69.2
40	81.5	63.5	63.0	63.5	64.2	64.5	63.7	64.0	64.7	63.2	64.5	64.7
50	77.7	62.7	64.5	63.7	64.0	64.5	63.2	64.7	64.7	64.2	64.7	65.0
63	76.0	63.0	63.7	63.0	65.0	63.0	65.2	64.2	66.2	62.5	64.5	66.0
80	74.0	61.5	62.0	61.5	65.7	64.7	65.0	64.2	68.7	64.0	64.2	69.0
100	69.0	64.2	60.5	60.5	70.0	68.7	68.0	67.7	75.2	68.2	66.0	73.0
125	72.0	69.5	64.0	62.7	72.5	71.5	70.2	70.7	77.0	70.5	67.7	75.7
160	71.7	77.2	76.2	66.5	76.2	74.5	76.5	76.5	80.7	75.5	73.2	79.5
200	80.5	61.5	65.0	76.2	83.2	79.7	87.2	87.5	86.2	83.7	82.2	85.0
250	77.2	86.2	69.5	72.2	82.7	81.5	88.5	89.7	86.7	87.0	80.5	86.2
315	81.2	89.2	77.0	78.2	92.2	79.7	89.5	92.5	85.7	89.0	78.0	85.2
400	85.0	87.5	80.5	84.7	78.7	79.7	86.5	91.2	81.7	86.2	74.5	83.0
500	85.7	87.5	82.0	85.0	79.7	81.2	86.0	90.7	81.7	84.5	78.5	82.5
630	85.0	92.0	81.2	83.7	80.7	81.7	95.2	99.7	86.2	92.7	81.2	84.2
800	89.5	88.0	85.5	84.0	85.7	88.0	92.2	92.5	89.0	87.7	84.2	87.5
1000	99.7	85.5	97.7	94.5	97.0	98.0	88.0	88.0	98.0	85.5	93.5	99.5
1250	99.2	86.0	82.2	94.5	94.0	97.2	88.2	88.0	94.7	86.7	91.5	99.0
1600	94.5	88.5	85.5	89.7	87.2	87.7	90.7	92.5	91.5	91.7	84.2	92.7
2000	92.7	92.2	87.7	89.5	86.5	83.0	93.5	96.7	88.5	92.7	81.2	89.0
2500	92.7	85.7	83.0	88.5	86.7	85.5	91.5	91.2	89.0	89.5	80.0	90.7
3150	94.0	84.7	85.2	87.2	83.5	84.5	87.2	89.7	87.0	87.7	80.5	90.7
4000	91.2	84.5	80.2	84.2	81.2	77.5	86.2	89.7	85.2	82.5	77.2	88.5
5000	91.2	86.2	77.2	83.2	79.7	78.0	84.7	90.5	83.7	82.5	75.2	89.2
6300	90.0	84.0	75.7	81.2	77.5	77.0	83.2	87.7	81.2	83.7	72.7	88.2
8000	88.5	85.0	73.7	80.0	75.5	74.2	82.0	87.5	79.5	82.2	70.5	86.0
10000	86.0	84.0	72.2	78.2	72.7	72.0	81.0	87.7	76.7	81.0	69.5	83.7
12500	84.5	82.2	72.5	79.0	70.5	70.2	80.0	85.5	74.0	78.7	68.0	82.2
16000	81.0	84.2	71.7	77.5	67.0	71.0	80.0	86.2	71.0	76.5	66.0	79.0
DBA	105.7	99.4	99.5	100.6	100.4	101.8	101.5	104.2	102.1	100.2	97.2	104.6

FREQUENCY HERTZ	15 **	16 **	22 **	21 **
25	70.5	72.5	70.0	70.2
31	70.0	69.0	70.0	68.7
40	64.2	64.0	64.2	63.2
50	63.5	64.0	64.5	63.7
63	61.2	63.5	65.2	63.7
80	62.2	62.0	65.7	61.5
100	62.5	64.0	68.5	61.5
125	65.5	67.7	71.7	63.5
160	65.0	72.7	77.0	70.5
200	66.7	79.0	83.0	81.0
250	66.7	84.5	83.0	67.0
315	67.5	86.0	81.0	68.2
400	68.5	84.2	79.7	70.7
500	75.0	84.7	80.7	71.7
630	78.5	87.5	80.7	75.2
800	78.2	85.0	84.7	76.0
1000	80.5	82.2	99.0	77.0
1250	78.5	83.2	93.5	78.0
1600	78.2	85.7	86.5	77.2
2000	74.0	89.2	85.2	76.2
2500	67.7	82.2	84.5	72.7
3150	69.7	86.2	84.0	76.5
4000	70.0	81.7	80.2	71.2
5000	68.0	79.2	79.0	71.7
6300	66.0	78.5	76.2	71.5
8000	65.2	76.2	73.0	69.7
10000	63.0	76.0	70.7	67.5
12500	63.0	76.0	67.2	67.7
16000	62.2	75.0	65.5	65.0
DBA	86.8	96.2	101.1	86.7

SPL OF OUTER CELLS

FREQUENCY HERTZ	1 **	2	3	4	5	6 **	12	18	24	30	36 **	35	34	33	32	31 **	25	19	13	7
25	68.7	70.0	69.7	80.7	70.5	69.5	70.2	70.2	70.0	71.2	71.0	68.7	69.0	71.7	70.5	72.0	72.0	72.2	71.0	68.7
31	68.5	67.0	67.7	76.7	69.5	68.0	67.2	70.0	69.2	66.0	68.0	67.5	69.5	67.7	71.2	69.0	67.7	68.2	68.0	68.5
40	63.7	63.7	64.2	72.0	63.7	64.7	64.5	65.0	64.5	64.5	62.5	65.2	63.5	64.2	64.5	65.0	64.0	63.2	64.5	64.2
50	63.7	62.2	63.7	68.7	64.2	62.0	63.2	65.7	64.2	64.0	64.2	66.0	64.2	62.7	65.5	64.0	63.5	66.0	63.2	63.5
63	62.5	61.5	63.0	65.0	63.2	61.2	61.5	62.2	62.2	62.7	62.5	68.0	64.7	63.7	66.2	61.7	62.2	63.5	64.2	63.2
80	60.5	61.2	61.7	63.7	60.5	62.2	63.0	62.0	63.2	65.5	62.5	72.2	63.5	67.5	67.5	63.0	63.2	63.0	62.2	62.2
100	60.5	60.5	60.7	63.2	60.5	60.5	65.2	64.0	63.7	69.2	64.7	77.2	66.7	72.7	71.2	68.0	65.0	65.2	64.0	60.5
125	65.7	63.7	65.7	68.5	65.0	62.0	68.0	66.0	66.5	71.0	66.2	80.0	69.5	74.0	75.5	70.2	67.5	68.5	67.0	62.0
160	71.2	77.5	69.0	75.0	65.5	66.2	75.0	66.2	71.5	75.7	66.7	84.2	74.5	78.2	80.0	75.5	67.5	75.0	70.5	71.7
200	65.5	64.7	78.5	71.0	71.5	76.0	82.2	71.0	81.5	86.5	73.7	87.2	79.5	83.5	86.0	86.7	73.0	79.7	76.2	66.0
250	70.5	69.7	71.0	74.7	72.2	70.5	83.5	68.0	69.7	85.2	70.2	88.5	85.5	83.5	86.2	86.2	70.0	83.7	83.2	70.0
315	78.5	78.0	76.0	79.0	80.0	78.2	86.2	67.2	69.5	82.0	69.5	87.7	89.2	81.5	84.7	89.0	70.5	86.5	86.7	77.2
400	84.5	82.5	83.7	83.0	86.2	85.5	85.0	69.2	70.0	78.7	71.2	85.7	86.2	82.7	82.5	87.2	74.2	85.7	84.0	81.7
500	86.0	84.7	83.0	84.5	87.2	86.0	84.7	75.2	77.0	77.7	75.2	84.2	84.7	82.0	81.7	87.0	77.2	83.7	85.2	83.5
630	83.2	81.7	84.5	82.0	86.7	85.5	88.7	81.7	82.2	84.7	82.2	88.5	94.5	85.7	86.7	96.0	79.0	89.0	85.5	80.0
800	87.2	86.2	87.2	89.5	87.2	86.7	87.0	77.5	78.0	88.5	81.2	90.2	86.5	90.2	88.0	89.7	78.7	87.7	83.7	83.7
1000	96.2	98.7	94.5	101.5	97.5	95.0	83.7	80.0	81.0	95.0	83.7	99.5	86.0	98.0	95.2	86.5	80.5	85.0	81.7	96.0
1250	85.5	84.2	93.0	87.0	93.5	94.2	83.7	81.0	81.2	94.5	83.5	100.5	85.5	97.5	95.0	88.5	79.2	83.0	79.0	81.7
1600	86.2	85.0	89.0	90.5	90.0	88.5	86.2	80.0	79.7	90.5	81.0	96.5	89.5	91.7	91.7	89.7	82.0	85.5	84.2	85.5
2000	89.2	89.0	90.7	89.2	91.0	90.5	87.7	74.2	73.7	85.0	76.5	91.0	93.5	84.5	87.5	92.0	76.5	90.0	88.5	85.7
2500	86.5	85.7	87.5	87.7	90.7	90.0	80.5	69.0	72.7	84.2	74.5	94.0	90.2	89.2	87.0	86.7	72.5	82.5	81.7	84.0
3150	85.5	86.0	89.2	89.5	90.0	87.7	82.0	69.0	75.2	84.5	72.2	95.0	84.5	88.7	86.7	85.2	77.7	81.5	79.7	85.5
4000	85.0	80.5	83.5	86.7	87.5	84.2	78.2	68.7	76.2	81.7	71.5	93.0	84.5	81.2	83.7	79.0	72.2	81.2	79.7	81.0
5000	84.5	79.2	82.0	87.2	88.5	83.5	77.2	68.5	72.7	79.0	70.5	93.5	81.2	80.7	83.2	77.0	71.7	79.2	77.5	78.7
6300	82.5	77.5	80.5	86.0	87.2	81.5	76.5	66.2	71.5	77.0	68.2	92.7	80.2	80.2	80.2	78.2	70.2	78.5	75.5	76.7
8000	82.5	75.7	78.7	83.5	86.7	80.2	76.0	67.5	70.5	73.7	66.7	91.0	81.0	78.5	77.7	80.5	68.5	77.2	76.5	75.2
10000	81.0	73.2	77.0	81.0	86.0	78.0	76.5	68.0	70.2	74.0	66.5	88.7	79.5	75.5	75.2	80.2	68.7	74.7	74.7	73.5
12500	79.0	72.5	76.2	80.2	83.0	76.5	78.0	63.5	68.2	71.0	66.5	86.7	81.2	72.5	71.5	78.2	68.5	74.2	77.7	77.0
16000	81.2	74.0	75.2	77.0	84.5	77.2	73.7	63.2	68.0	70.0	65.7	84.0	79.5	69.2	69.5	76.0	70.7	75.2	77.2	76.2
DBA	99.7	100.5	100.4	103.5	102.5	101.0	95.7	87.9	89.1	100.1	90.3	106.7	100.1	102.8	101.1	100.0	89.0	96.6	94.7	98.3

Appendix D

SUMMARY OF TESTS CONDUCTED ON HIGH-SPEED AND LOW-SPEED FANS

TEST: High-Speed Fan

Test Identification No.
7-1-48

TEST CONFIGURATION	STAGGER ANGLE	INSTRUMENT STATION	AZIMUTH POSITION	%RPM	% WEIGHT FLOW & RUN NO. 70	80	90	95	100	105	110	INLET DISTORTION CONFIGURATION
	56.08	6	P	100	4				3		2	
	"	"	"	"				7	5	6		
	"	"	T	"	10				9		8	
	"	"	S	"	13				12		11	
	"	"	B	"	16				15		14	
	"	5	P	"					18		17	
	"	4	"	"	22				21		20	

TEST: Low-Speed Fan No. 1

Test Identification No.
7-2-48

TEST CONFIGURATION	STAGGER ANGLE	INSTRUMENT STATION	AZIMUTH POSITION	%RPM	% WEIGHT FLOW & RUN NO. 70	80	90	95	100	105	110	INLET DISTORTION CONFIGURATION
	40.8	6	P	100	27	26	25	24	23			
	"	"	"	90		30	29	28				
	"	"	T	100	33			32	31			
	"	"	"	90				34				
	35.4	"	S	100				37	36	35		
	"	"	"	90					38			
	"	"	B	100				41	40	39		
	"	"	"	90					42			
	"	"	T	100				45	44	43		
	"	"	"	90					46			
	"	"	P	100	53	52	51	50	49	48	47	
	"	"	"	90		56	55		54			
	"	4	"	100	63	62	61	60	59	58	57	
	"	"	"	90		66	65		64			
	"	"	T	100				69	68	67		
	"	"	"	90					70			
	"	"	B	100				73	72	71		
	"	"	"	90					74			

TEST: Low-Speed Fan No. 1

Test Identification No.
7-2-48

TEST CONFIGURATION	STAGGER ANGLE	INSTRUMENT STATION	AZIMUTH POSITION	%RPM	% WEIGHT FLOW & RUN NO. 70	80	90	95	100	105	110	INLET DISTORTION CONFIGURATION
	35.4	4	S	100				77	76	75		
	"	"	"	90					78			
Station 7 Totals	"	4/7	"	100	79	79	79		79		79	
"	"	"	"	90		80	80		80			
Honeycomb Out	"	"	"	100					82			
"	32.9	6	P	100	86	85	84		83			
"	"	"	"	90					87			
"	"	"	"	70	90	89			88			
"	"	"	T	100			92		91			
"	"	"	"	90					93			
"	"	"	"	70					94			
"	"	"	S	100				96	95			
"	"	"	"	90					97			
"	"	"	"	70					98			
"	"	"	B	100			100		99			
"	"	"	"	90					101			
"	"	"	"	70					102			
"	40.8	"	"	100	106			105	104	103		

TEST: High-Speed Fan

Test Identification No.
7-1-48

TEST CONFIGURATION	STAGGER ANGLE	INSTRUMENT STATION	AZIMUTH POSITION	%RPM	% WEIGHT FLOW & RUN NO. 70	80	90	95	100	105	110	INLET DISTORTION CONFIGURATION
Honeycomb Out	40.8	6	R	90				107				
	"	"	S	100	111			110	109	108		
	"	"	"	90				112				
	"	"	T	100	116			115	114	113		
	"	"	"	90				117				
	"	"	P	100	121			120	119	118		
	"	"	"	90				122				
	45.2	"	"	100	127	126	125		124		123	
	"	"	"	70	130	129			128			
	"	"	T	100			133		132		131	
	"	"	"	70					134			
	"	"	S	100	138		137		136		135	
	"	"	B	100	142		141		140		139	
	35.4	4	P	100	148	147	146	145	144	143		
INLET HONEYCOMB INSTALLED												
	"	"	T	"	152		151		150	149		
	"	"	S	"	156		155		154	153		
	"	"	B	"	160		159		158	157		

TEST: Low-Speed Fan No. 1

Test Identification No.
7-2-48

TEST CONFIGURATION	STAGGER ANGLE	INSTRUMENT STATION	AZIMUTH POSITION	%RPM	% WEIGHT FLOW & RUN NO. 70	80	90	95	100	105	110	INLET DISTORTION CONFIGURATION
Exit Honeycomb Out	35.4	4	B	100	160		159		158	157		
Inlet Honeycomb In												
"	"	6	P	"	166	165	164	163	162	161		
"	"	"	T	"	170		169		168	167		
"	"	"	S	"	174		173		172	171		
"	"	"	B	"	178		177		176	175		
"	"	"	"	90					179			
"	"	"	"	80					180			
"	"	"	"	75					181			
"	"	"	"	50					182			
"	"	5	B	100	186		185		184	183		
"	"	"	P	"	192	191	190	189	188	187		
"	"	"	T	"	196		195		194	193		
"	"	"	S	"	200		199		198	197		
"	52.3	"	"	"	203		202		201			
"	"	4	"	"	209	208	207	206	205	204		
"	"	6	"	"	215	214	213	212	211	210		
"	40.8	6/7	"	"	218		217		216			
"	"	6	"	"	221		220		219			

TEST: Low-Speed Fan No. 1

Test Identification No.
7-2-48

TEST CONFIGURATION	STAGGER ANGLE	INSTRUMENT STATION	AZIMUTH POSITION	%RPM	% WEIGHT FLOW & RUN NO. 70	80	90	95	100	105	110	INLET DISTORTION CONFIGURATION
Exit Honeycomb Out Inlet Honeycomb In	40.8	6	S	100	224		223		222			H
"	"	"	"	"	227		226		225			V
"	"	"	B	"	230		229		228			V
"	"	"	"	"	233		232		231			H
"	"	"	"	"	236		235		234			–
"	"	6/7	"	"	239		238		237			–
"	"	"	P	"	244	243	242	241	240			–
"	"	6	"	"	249	248	247	246	245			–
"	"	"	"	"	254	253	252	251	250			H
"	"	"	"	"	259	258	257	256	255			V
"	"	"	T	"	262		261		260			V
"	"	"	"	"	265		264		263			H
"	"	"	"	"	268		267		266			–
"	"	6/7	"	"	271		270		269			–
"	"	5	"	"	274		273		272			H
"	"	4	"	"	277		276		275			"
"	"	"	S	"	280		279		278			"
"	"	5	"	"	283		282		281			"

TEST: Low-Speed Fan No. 1

Test Identification No.
7-2-48

TEST CONFIGURATION	STAGGER ANGLE	INSTRUMENT STATION	AZIMUTH POSITION	%RPM	% WEIGHT FLOW & RUN NO. 70	80	90	95	100	105	110	INLET DISTORTION CONFIGURATION
Exit Honeycomb Out Inlet Honeycomb In	40.8	5	S	100	286		285		284			H
"	"	4	"	"	289		288		287			"
"	"	"	P	"	294	293	292	291	290			–
"	"	"	"	"	299	298	297	296	295			H
"	"	5	"	"	304	303	302	301	300			"
"	"	"	"	"	309	308	307	306	305			–
"	"	6	"	"	314	313	312	311	310		319	
"	"	"	"	90					315		320	
"	"	"	"	80					316		321	
"	"	"	"	75					317		322	
"	"	"	"	50					318		323	
"	88.4	4/7	–	100					324			
"	"	6	P	"					325			
"	"	"	"	50					326			
"	62.9	"	"	100			329		328			327 (at 120)
Modified Contraction	"	6/7	"	"			330		330		330	
"	"	6/4	"	"			331		331		331	
"	"	6	"	"			334		333		332	

TEST: Low-Speed Fan No. 1

Test Identification No.
7-2-48

TEST CONFIGURATION	STAGGER ANGLE	INSTRUMENT STATION	AZIMUTH POSITION	%RPM	% WEIGHT FLOW & RUN NO. 70	80	90	95	100	105	110	INLET DISTORTION CONFIGURATION
Modified Contraction	62.9	5	P	100			337		336		335	–
"	"	4	"	"			340		339		338	–
"	40.8	"	"	"	344		343	342	341			
"	"	"	"	90					345			
"	"	"	"	75					346			
"	"	"	"	50					347			
"	"	"	"	100	351		350	349	348			A
"	"	"	"	90					352			
"	"	"	"	75					353			
"	"	"	"	50					354			"
"	"	"	"	100	358		357	356	355			B
"	"	"	"	90					359			"
"	"	"	"	75					360			"
"	"	"	"	50					361			"
"	"	5/4	"	100	362		362	362	362			"
"	"	"	"	"	363		363	363	363			A
"	"	"	"	"	364		364	364	364			–
"	"	5/7	"	"	365		365	365	365			–

TEST: Low-Speed Fan No. 1

Test Identification No. 7-2-48

TEST CONFIGURATION	STAGGER ANGLE	INSTRUMENT STATION	AZIMUTH POSITION	%RPM	% WEIGHT FLOW & RUN NO. 70	80	90	95	100	105	110	INLET DISTORTION CONFIGURATION
Modified Contraction	40.8	5/7	P	100	366		366	366	366			A
"	"	"	"	"	367		367	367	367			B
"	"	5	"	"	371		370	369	368			"
"	"	"	"	"	375		374	373	372			A
"	"	"	"	"	379		378	377	376			-
"	"	6	"	"	383		382	381	380			-
"	"	"	"	"	384		385	386	387			A
"	"	"	"	"	391		390	389	388			B
"	"	"	T	"	395		394	393	392			B
"	"	"	"	"	399		398	397	396			A
"	"	"	"	"	403		402	401	400			-
"	"	5	"	"	404		405	406	407			-
"	"	"	"	"	411		410	409	408			A
"	"	"	"	"	412		413	414	415			B
"	"	4	"	"	419		418	417	416			"
"	"	"	"	"	423		422	421	420			A
"	"	"	"	"	427		426	425	424			-
"	"	"	S	"	431		430	429	428			-

TEST: Low-Speed Fan No. 1

Test Identification No.
7-2-48

TEST CONFIGURATION	STAGGER ANGLE	INSTRUMENT STATION	AZIMUTH POSITION	%RPM	% WEIGHT FLOW & RUN NO. 70	80	90	95	100	105	110	INLET DISTORTION CONFIGURATION
Modified Contraction	40.8	4	S	100	432		433	434	435			A
"	"	"	"	"	439		438	437	436			B
"	"	5	"	"	443		442	441	440			"
"	"	"	"	"	447		446	445	444			A
"	"	"	"	"	451		450	449	448			-
"	"	4	"	"					452			C
"	"	7	"	"					453			"
"	"	6	B	"					454			C
"	"	4/5	"	"					455			D_5
"	"	"	"	"					456			D_7
"	"	"	"	"					457			D_9
"	"	"	"	"					458			D_{10}
"	"	7/5	"	"					459			D_9
"	'	5	"	"					460			"
"	"	4	"	"					461			"
"	"	6	"	"					462			"
"	"	"	T	"					463			"
"	"	5	"	"					464			"

TEST: Low-Speed Fan No. 1

Test Identification No.
7-2-48

TEST CONFIGURATION	STAGGER ANGLE	INSTRUMENT STATION	AZIMUTH POSITION	%RPM	% WEIGHT FLOW & RUN NO. 70	80	90	95	100	105	110	INLET DISTORTION CONFIGURATION
Modified Contraction	40.8	4	T	100					465			D_9
"	38.0	"	"	"	469			468	467	466		-
"	"	5	"	"	473			472	471	470		-
"	"	6	"	"	477			476	475	474		-
"	"	"	P	"	481			480	479	478		-
"	"	7/5	"	"					482			-
"	"	"	"	"				483				D_8
"	"	4/5	"	"				484				"
"	"	"	"	"					485			-
"	"	6	"	"			488		487	486		-
"	"	"	B	"			491		490	489		-
"	"	"	S	"			494		493	492		-
"	"	4	B	"					495			-
"	"	"	"	"				496				D_8
"	"	5	"	"				497				"
"	"	6	"	"				498				"
"	"	"	T	"				499				"
"	"	5	"	"				500				"

TEST: Low-Speed Fan No. 1

Test Identification No. 7-2-48

TEST CONFIGURATION	STAGGER ANGLE	INSTRUMENT STATION	AZIMUTH POSITION	%RPM	% WEIGHT FLOW & RUN NO. 70	80	90	95	100	105	110	INLET DISTORTION CONFIGURATION
Modified Contraction	38.0	4	T	100				501				D_8
"	"	"	P	"					502			–
"	"	"	S	"					503			–
"	"	6	T	"			504					D.S.
"	"	"	S	"			505					"
"	"	"	B	"			506					"
"	"	"	P	"			507					"
"	"	4	B	"			508					"
"	"	4 rakes	–	"			509					"
"	"	7 "	–	"			510					